



# A process based model of cohesive sediment resuspension under bioturbators' influence

Francesco Cozzoli<sup>a,d,\*</sup>, Vojsava Gjoni<sup>a</sup>, Michela Del Pasqua<sup>a</sup>, Zhan Hu<sup>b,h,\*\*</sup>, Tom Ysebaert<sup>c,d</sup>, Peter M.J. Herman<sup>e,f</sup>, Tjeerd J. Bouma<sup>d,g</sup>

<sup>a</sup> Dipartimento di Scienze e Tecnologie Biologiche ed Ambientali, University of the Salento – 73100, Lecce, Italy

<sup>b</sup> School of Marine Science, Sun Yat-sen University, 510275 Guangzhou, China

<sup>c</sup> Wageningen Marine Research, Wageningen University and Research, P.B. 77, 4400 AB Yerseke, The Netherlands

<sup>d</sup> Department of Estuarine and Delta Systems, Royal Netherlands Institute of Sea Research (NIOZ) and Utrecht University, 4401 NT Yerseke, The Netherlands

<sup>e</sup> Department of Hydraulic Engineering, Delft University of Technology, 2628 CN, P.O. Box 5048, 2600 GA, Delft, The Netherlands

<sup>f</sup> Deltares, P.O. Box 177, 2600 MH, Delft, The Netherlands

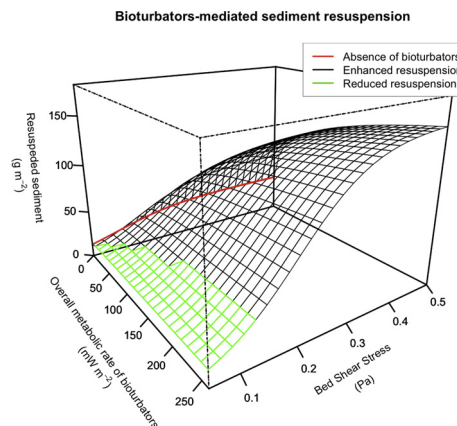
<sup>g</sup> Department of Physical Geography, Utrecht University, P.O. Box 80.115, 3508 TC, Utrecht, The Netherlands

<sup>h</sup> Southern Laboratory of Ocean Science and Engineering (Guangdong, Zhuhai), Zhuhai 519000, China

## HIGHLIGHTS

- Benthic infauna affects sediment erodibility via their bioturbating activities.
- Metabolic size scaling allows one to derive general patterns of biotic effect on erosion.
- The effect of different bioturbators was compared by using recirculating flumes.
- The effect of bioturbators on sediment erosion can be described by their metabolism.

## GRAPHICAL ABSTRACT



## ARTICLE INFO

### Article history:

Received 13 December 2018

Received in revised form 9 February 2019

Accepted 6 March 2019

Available online 14 March 2019

Editor: Sergi Sabater

### Keywords:

Bioturbation

## ABSTRACT

Macrozoobenthos may affect sediment stability and erodibility via their bioturbating activities, thereby impacting both the short- and long-term development of coastal morphology. Process-based models accounting for the effect of bioturbation are needed for the modelling of erosion dynamics.

With this work, we explore whether the fundamental allometric principles of metabolic activity scaling with individual and population size may provide a framework to derive general patterns of bioturbation effect on cohesive sediment resuspension. Experimental flumes were used to test this scaling approach across different species of marine, soft-sediment bioturbators. The collected dataset encompasses a range of bioturbator functional diversity, individual densities, body sizes and overall population metabolic rates. Measurements were collected across a range of hydrodynamic stress from 0.02 to 0.25 Pa.

\* Correspondence to: F. Cozzoli, Dipartimento di Scienze e Tecnologie Biologiche ed Ambientali, Centro Ecotekne, Pal. B S.P. 6 Lecce – Monteroni, 73100 Lecce, Italy.

\*\* Corresponding author.

E-mail addresses: [francesco.cozzoli@unisalento.it](mailto:francesco.cozzoli@unisalento.it) (F. Cozzoli), [huzh9@mail.sysu.edu.cn](mailto:huzh9@mail.sysu.edu.cn) (Z. Hu).

Sediment resuspension  
Annular flumes  
Metabolism  
Process-based model

Overall, we observed that bioturbators are able to slightly reduce the sediment resuspension at low hydrodynamic stress, whereas they noticeably enhance it at higher levels of stress. Along the whole hydrodynamic stress gradient, the quantitative effect of bioturbators on sediment resuspension can be efficiently described by the overall metabolic rate of the bioturbating benthic communities, with significant variations across the bioturbators' taxonomic and functional diversity. One of the tested species (the gallery-builder Polychaeta *Hediste diversicolor*) had an effect that was partially deviating from the general trend, being able to markedly reduce sediment resuspension at low hydrodynamic stress compared to other species. By combining bioturbators' influence with hydrodynamic force, we were able to produce a process-based model of biota-mediated sediment resuspension.

© 2019 Elsevier B.V. All rights reserved.

## 1. Introduction

Organisms may physically change the abiotic environment, either by their structures (*i.e.*, autogenic ecosystem engineering) or by their activity (*i.e.*, allogenic ecosystem engineering) (Jones et al., 1994; Jones et al., 1997). By engineering their environment, biotic agents can exacerbate or dampen ongoing physical trends (Crooks, 2002). As a noticeable case, sediment dynamics originate from the physical interaction between the drag force of the water flow and the sediment particles (Allen, 1985; Winterwerp and van Kesteren, 2004; Fagherazzi and Wiberg, 2009; Friedrichs, 2011; Zhou et al., 2015), but they may be heavily modulated by biotic agents (Widdows and Brinsley, 2002; Le Hir et al., 2007; Grabowski et al., 2011; Friedrichs, 2011). Macrozoobenthos living inside the sediment are ecosystem engineers in the sense that they may alter the bottom sediment properties with their bioturbation activities (Le Hir et al., 2007). The surface roughness generated by the bioturbators reworking the sediment may dampen the near bottom hydrodynamics and shelter the sediment surface, preventing resuspension (Friedrichs et al., 2009; Friedrichs, 2011). Nevertheless, bioturbators generally make the sediment less resistant to erosion by loosening it with their activities (Willows et al., 1998; Ciutat et al., 2007; Montserrat et al., 2008; Volkenborn et al., 2009; van Prooijen et al., 2011; Rakotomalala et al., 2015; Cozzoli et al., 2018a; Joensuu et al., 2018). The effect of bioturbators on cohesive sediment resuspension impacts the short- and long-term development of coastal morphology (Le Hir et al., 2007; Orvain et al., 2012; Winterwerp et al., 2018), and should hence be taken into account when forecasting the evolution of landscapes and ecosystems (Solan et al., 2004a; Orvain, 2005; Orvain et al., 2012; Bouma et al., 2014; Queirós et al., 2015; Nasermoaddeli et al., 2018). Beyond coastal morphology, sediment resuspension is related to the oxygenation and the transfer of particles and nutrients within the sediment layers and from the sediment surface to the water column (Ubertaini et al., 2012). For this reason, bioturbation may have a broad influence on biogeochemical cycles (Solan et al., 2004a; Quintana et al., 2015; Thomsen et al., 2017; Zhang et al., 2017; Wrede et al., 2018), pollutants diffusion (Kupryianchuk et al., 2013) species coexistence (Mermillod-Blondin and Lemoine, 2010; David et al., 2016; Chen et al., 2017) and aquatic food webs (Saint-Béat et al., 2014; Abrantes et al., 2014; Zou et al., 2016).

Bioturbators are characterized by high taxonomic and functional diversity (Holtmann et al., 1996). Five main types of functional bioturbation groups exhibiting different modes of sediment mixing may be distinguished: the biodiffusers, upward conveyors, downward conveyors, regenerators and gallery-diffusers (Lee and Swartz, 1980; Solan et al., 2004b; Queirós et al., 2013). Species-specific trait-based models proved to have good performance in the quantitative prediction of the intensity of sediment reworking (Solan et al., 2004a, 2004b; Queirós et al., 2013; Queirós et al., 2015) and of closely related processes as bioirrigation (Wrede et al., 2018). However, formulating a general mechanistic framework to quantify bioturbation processes based on species-specific functional traits remains difficult due to the high variation in bioturbators' species distribution and functional behaviour

(Queirós et al., 2013). According to van Prooijen et al. (2011), widely applicable models of bio-mediated physical dynamics should be based on a set of formulations derived from generally valid (*i.e.* not site-specific or species-specific) physicochemical and biological laws, each formulation representing a (sub)process. The advantage of such process-based models is that sub-processes can be combined and results can be extrapolated, as general laws should hold everywhere.

Body size allometry is one approach that has allowed for development of important ecological generalizations since almost all the fundamental traits of organisms vary predictably with their size [*e.g.* (Peters, 1983; De Roos et al., 2003; Gaston and Blackburn, 2000; Brown et al., 2004; Marquet et al., 2005)]. In particular, the body size of organisms shows a positive allometric relationship with their rate of biological processing of energy and material, *i.e.* the metabolic rate (Kleiber, 1932; Peters, 1983; Gaston and Blackburn, 2000; Kooijman, 2000; Brown et al., 2004; Savage et al., 2004; Sousa et al., 2008). The individual metabolic rate feeds other key individual (*e.g.* development, reproduction, locomotion, oxygen and food intake), population (*e.g.* growth rate, carrying capacity), community (*e.g.* diversity, rate of interaction) and ecosystem (*e.g.* biomass production, trophic dynamics) processes, so that it has been proposed as a holistic measure of the 'pace of life' (Brown et al., 2004). Ecological metabolic theories [*e.g.* (Brown et al., 2004; Kooijman, 2000)] can be used to link ecological outcomes to biophysical processes by using the first principles of physics, chemistry, and biology that govern the organismic processing of energy and material.

At the individual level, the metabolic rate of bioturbators has been proposed as a synthetic descriptor for the intensity of bioturbation (Cozzoli et al., 2018a) because of its positive relation with the intensity of the physiological activities involved in the sediment bioturbation as respiration [*e.g.* burrow ventilation, valves shacking (Kristensen, 1983; Ciutat et al., 2007)], feeding [*e.g.* swallowing, excretion and disruption of the sediment to extract organic particles (Zebe and Schiedek, 1996; van Prooijen et al., 2011)] and moving [*e.g.* digging, crawling (Friedrichs et al., 2009)]. Mesocosm experiments performed at constant hydrodynamic stress showed that the effect of individual bioturbation activity on sediment resuspension can be scaled to the population level (Cozzoli et al., 2018a). This concept is also supported by the recent work of Wrede et al. (2018), demonstrating that size scaling rules of metabolic rates can provide a base to predict the intensity of bioirrigation at the community level.

With this study, we propose a process-based model [*sensu van Prooijen et al., 2011*] of bioturbators-mediated cohesive sediment resuspension. For this purpose, we explored the potential of the bioturbators' metabolic rate as a general descriptor of the biological influences on sediment resuspension in relation to changes in hydrodynamic energy, which is the main physical driver of sediment dynamics (Allen, 1985; Winterwerp and van Kesteren, 2004; Fagherazzi and Wiberg, 2009; Friedrichs, 2011; Zhou et al., 2015). Given that: *i*) sediment reworking at the individual level usually results from the bioturbator respiration, feeding, and moving activities; *ii*) these activities are fuelled from the individual metabolic rate, of which the individual size is a proxy; *iii*) multiple individuals bioturbating the sediment cumulate their metabolic rates and their effect on sediment resuspension; we hypothesised

that changes *per area* of suspended cohesive sediment through an hydrodynamic energy gradient are fundamentally related to changes in the overall metabolic rate of the bioturbating population, rather than to specificities in the sediment reworking modality. To test the hypothesis in controlled conditions, we performed a series of mesocosm experiments by using annular recirculating flumes. To investigate if the overall activity of the bioturbating population (approximated as the population basal metabolic rate) is indeed the main driver explaining variations in the mass of suspended sediment, we compared the quantitative effect on sediment resuspension of several common species of bioturbators, characterized by different functional behaviour (Table 1).

## 2. Material & methods

### 2.1. Experimental design

We used mesocosm recirculating annular flumes to mimic the environmental conditions of the intermediate - upper part of an intertidal flat (*i.e.* muddy sediment, low to intermediate hydrodynamic stress), where bioturbators are typically most abundant (Pearson and Rosenberg, 1978; Nilsson and Rosenberg, 2002) and most effective in enhancing sediment resuspension (Orvain et al., 2012). The mesocosm approach allowed us to test the hypothesis under controlled conditions, excluding variation in both physical factors [*e.g.* sediment grain size, cohesiveness and compaction (van Prooijen and Winterwerp, 2010)], and

in physiological or behavioural changes of the bioturbation activity in response to environmental cues [*e.g.* acidification (Yvon-Durocher et al., 2012; Ong et al., 2017); temperature (Verdelhos et al., 2015a); salinity (Verdelhos et al., 2015b); food availability (Maire et al., 2006)]. Variations in the amount of suspended sediment ( $R_{TOT}$ ,  $g\ m^{-2}$ ) were used as a measure of the bioturbation effect on sediment erodibility along a gradient of hydrodynamic stress.

The tested combinations of bioturbator body sizes and densities were selected in a way to cover the natural range of each analysed species [*e.g.* (Zebe and Schiedek, 1996; Holtmann et al., 1996; Degraer et al., 2006)], *i.e.* to represent commonly observed high densities and large individual sizes and low densities and small individual size, with values within these end points as well. The availability of field collected and homogeneously sized experimental organisms was limited and not always sufficient to fully cover a complete factorial design, crossing all species, sizes and density levels. We did not run experiments with very high densities of large individuals (*i.e.* overall biomass  $> 120\ g\ AFDW\ m^{-2}$ ) due to saturation of the surface of the experimental flumes. We also avoided running experiments with very low densities of smaller individual (*i.e.* overall biomass  $< 0.6\ g\ AFDW\ m^{-2}$ ) because preliminary observations did not show any detectable biotic effect on sediment resuspension below this threshold. Respecting these conditions, we managed to collect a dataset encompassing a range of bioturbators taxonomic (8 species) and functional diversity (from shallow to deep bioturbators), individual densities (13 to 6366 Ind.  $m^{-2}$ )

**Table 1**  
Table of treatments (ordered by the individual size of the bioturbators) and estimates for the asymptote  $a$  (suspended sediment,  $R_{TOT}$ ,  $g\ m^{-2}$ ), the midterm  $b$  (Bed Shear Stress, BSS, Pa) and the constant  $c$  (Pa) estimated from the mixed logistic model  $R_{TOT} = a_{BIO}/(1 + e^{(b - BSS)/c})$  for each treatment.

|                                | Individual size | Number of individuals in the flume | Density of individuals | Overall metabolic rate | Asymptote   | Midterm | Constant |
|--------------------------------|-----------------|------------------------------------|------------------------|------------------------|-------------|---------|----------|
| Abbreviation                   | M               | N                                  | D                      | $R_{TOT}$              | a           | b       | c        |
| Unit                           | mg AFDW         | N of Ind.                          | N of Ind. $m^{-2}$     | $mW\ m^{-2}$           | $g\ m^{-2}$ | Pa      | Pa       |
| Species                        |                 |                                    |                        |                        |             |         |          |
| Defaunated control             | 0               | 0                                  | 0                      | 0                      | 41          | 0.08    | 0.07     |
| <i>Corophium volutator</i>     | 0.25            | 500                                | 3183                   | 9                      | 83          | 0.09    | 0.07     |
| <i>Corophium volutator</i>     | 0.25            | 750                                | 4775                   | 13                     | 104         | 0.12    | 0.07     |
| <i>Corophium volutator</i>     | 0.25            | 1000                               | 6366                   | 17                     | 130         | 0.11    | 0.07     |
| <i>Cerastoderma edule</i>      | 11              | 15                                 | 96                     | 6                      | 66          | 0.14    | 0.07     |
| <i>Cerastoderma edule</i>      | 11              | 30                                 | 191                    | 13                     | 72          | 0.13    | 0.07     |
| <i>Cerastoderma edule</i>      | 11              | 60                                 | 382                    | 26                     | 106         | 0.17    | 0.07     |
| <i>Abra alba</i>               | 14              | 7                                  | 45                     | 4                      | 55          | 0.13    | 0.07     |
| <i>Abra alba</i>               | 14              | 15                                 | 95                     | 8                      | 55          | 0.12    | 0.07     |
| <i>Scrobicularia plana</i>     | 15              | 10                                 | 64                     | 5                      | 80          | 0.12    | 0.07     |
| <i>Scrobicularia plana</i>     | 15              | 60                                 | 382                    | 32                     | 98          | 0.11    | 0.07     |
| <i>Hediste diversicolor</i>    | 20              | 50                                 | 318                    | 26                     | 89          | 0.23    | 0.07     |
| <i>Hediste diversicolor</i>    | 20              | 100                                | 636                    | 52                     | 148         | 0.25    | 0.07     |
| <i>Hediste diversicolor</i>    | 20              | 150                                | 955                    | 79                     | 114         | 0.24    | 0.07     |
| <i>Arenicola marina</i>        | 22              | 5                                  | 32                     | 3                      | 40          | 0.16    | 0.07     |
| <i>Arenicola marina</i>        | 22              | 10                                 | 64                     | 6                      | 56          | 0.13    | 0.07     |
| <i>Arenicola marina</i>        | 22              | 15                                 | 95                     | 9                      | 106         | 0.2     | 0.07     |
| <i>Arenicola marina</i>        | 22              | 20                                 | 127                    | 12                     | 61          | 0.14    | 0.07     |
| <i>Limecola balthica</i>       | 30              | 5                                  | 32                     | 5                      | 46          | 0.09    | 0.07     |
| <i>Limecola balthica</i>       | 30              | 10                                 | 64                     | 9                      | 55          | 0.13    | 0.07     |
| <i>Limecola balthica</i>       | 30              | 30                                 | 191                    | 27                     | 131         | 0.21    | 0.07     |
| <i>Limecola balthica</i>       | 30              | 60                                 | 382                    | 54                     | 136         | 0.19    | 0.07     |
| <i>Cerastoderma edule</i>      | 101             | 5                                  | 32                     | 11                     | 113         | 0.19    | 0.07     |
| <i>Cerastoderma edule</i>      | 101             | 10                                 | 64                     | 23                     | 86          | 0.14    | 0.07     |
| <i>Cerastoderma edule</i>      | 101             | 20                                 | 127                    | 45                     | 79          | 0.14    | 0.07     |
| <i>Cerastoderma edule</i>      | 101             | 40                                 | 255                    | 90                     | 115         | 0.15    | 0.07     |
| <i>Ruditapes philippinarum</i> | 128             | 5                                  | 32                     | 13                     | 76          | 0.18    | 0.07     |
| <i>Scrobicularia plana</i>     | 171             | 10                                 | 64                     | 33                     | 100         | 0.14    | 0.07     |
| <i>Arenicola marina</i>        | 210             | 5                                  | 323                    | 19                     | 58          | 0.16    | 0.07     |
| <i>Arenicola marina</i>        | 210             | 10                                 | 64                     | 39                     | 126         | 0.22    | 0.07     |
| <i>Arenicola marina</i>        | 210             | 15                                 | 95                     | 58                     | 75          | 0.11    | 0.07     |
| <i>Arenicola marina</i>        | 210             | 20                                 | 127                    | 77                     | 111         | 0.17    | 0.07     |
| <i>Cerastoderma edule</i>      | 616             | 2                                  | 13                     | 17                     | 51          | 0.11    | 0.07     |
| <i>Cerastoderma edule</i>      | 616             | 5                                  | 32                     | 43                     | 88          | 0.13    | 0.07     |
| <i>Cerastoderma edule</i>      | 616             | 10                                 | 64                     | 87                     | 134         | 0.19    | 0.07     |
| <i>Cerastoderma edule</i>      | 616             | 30                                 | 191                    | 261                    | 192         | 0.18    | 0.07     |
| <i>Arenicola marina</i>        | 1120            | 5                                  | 32                     | 77                     | 137         | 0.21    | 0.07     |
| <i>Arenicola marina</i>        | 1120            | 10                                 | 64                     | 155                    | 70          | 0.14    | 0.07     |
| <i>Arenicola marina</i>        | 1120            | 15                                 | 95                     | 232                    | 143         | 0.17    | 0.07     |

and individual body sizes (0.25 to 1120 mg Ash Free Dry Weight, AFDW), for a total of 38 unique combinations of species, size and density plus two defaunated controls (Table 1). Each treatment always used homogeneously sized individuals of a single species and was replicated twice. The overall bioturbator population basal metabolic rates, expressed as a linear combination of individual metabolic rates at the experimental temperature and density of individuals ( $I_{TOT}$ ,  $mW m^{-2}$ ), were estimated for each treatment according to the empirical model for aquatic macroinvertebrates respiration of Brey (2010) and ranged from 3 to 260  $mW m^{-2}$  (Table 1).

A portion of the dataset (observations collected at bed shear stress of 0.18 Pa on a subset of species) has been published to investigate the biotic effect on sediment resuspension at a fixed current velocity in Cozzoli et al. (2018a). The complete dataset is available as Appendix of this paper (Appendix A and to the OSF repository at <https://dx.doi.org/10.17605/OSF.IO/JU4DH>).

## 2.2. Model organisms

For our measurements we used a range of bioturbators that commonly coexist on temperate muddy intertidal flats (Holtmann et al., 1996; Degraer et al., 2006), although with slightly different preferences for the composition of the inhabiting sediment (Anderson, 2008; Cozzoli et al., 2013). They are all endemic to the North Atlantic Ocean with the exception of *Ruditapes philippinarum*, a non-indigenous species native of the Indian and Pacific Oceans that is rapidly expanding in the North Sea (Humphreys et al., 2015). Cumulatively, the species accounted for in this study make up 60% of the macrozoobenthos intertidal biomass in temperate estuaries such as the Westerschelde and Oosterschelde (SW Delta, the Netherlands), and they can locally reach almost 100% (Cozzoli et al., 2013). The model species were selected as explained below:

- Shallow-burrowing Bivalvia represented by obligatory suspension feeder *Cerastoderma edule* (Linnaeus, 1758). *C. edule* makes shallow perturbations (shells usually emerge from the sediment surface) in the sediment by crawling, shaking valves and producing pelleted pseudo-faeces, (Flach, 1996). This species can reach a relatively large individual size (up to 600 mg Ash Free Dry Weight, AFDW) and high density (adult density up to 500  $Ind. m^{-2}$  along the North Sea coasts) (Cozzoli et al., 2014). Several field and laboratory studies showed that *C. edule* destabilizes the cohesive sediment making it more erodible [e.g. (Flach, 1996; Ciutat et al., 2007; Montserrat et al., 2009; Li et al., 2017)].
- Intermediate burrowing Bivalvia that live in the sediment at a depth of 3–10 cm, represented by facultative suspension feeder *Abra alba* (Wood, 1802), *Scrobicularia plana* (da Costa, 1778), *Limecola balthica* (Linnaeus, 1758) and *Ruditapes philippinarum* (Adams and Reeve, 1850). While differing in the maximal adult size [from 50 mg AFDW for *L. balthica* and *A. alba* up to 300 mg AFDW for *S. plana*, (Swartz, 1991)], these organisms share common lifestyles, and modes of feeding and mobility (Purchon, 1997; Queirós et al., 2013), and have a similar effect on sediment resuspension (Cozzoli et al., 2018a). They often behave as surface deposit feeders, by inhaling sediment through their siphons and depositing pseudo-faeces (Zwarts et al., 1994; Purchon, 1997). By doing so, they disrupt the sediment surface and increase the erodibility (Willows et al., 1998; Widdows et al., 1998; Orvain, 2005; Sgro et al., 2005; van Prooijen et al., 2011).
- Intermediate-burrowing Amphipoda that live in U-shaped burrows represented by *Corophium volutator* (Pallas, 1776). These small bioturbators (average weight 0.25 mg AFDW) may reach very high densities (up to 15,000  $Ind m^{-2}$ ) in the upper part of the tidal flats (De Backer et al., 2011). Burrows are ca. 5 cm deep (Flach, 1996) and their openings can protrude 1 to 1.5 mm above the sediment surface, especially in fine mud (Meadows and Reid, 1966; Meadows et al., 1990). When acting as filter feeder, *C. volutator* pump large amounts

of water through the burrows and contribute actively to sediment resuspension (De Backer et al., 2011). If suspended phytoplankton is not abundant, surface deposit feeding is the main feeding mode, and then particles are predominantly gathered by scraping the sediment surface with the enlarged second antennae (Meadows and Reid, 1966). Its bioturbation effect on sediment stability is variable (Le Hir et al., 2007). For instance, both negative (Meadows and Tait, 1989), positive (Gerdol and Hughes, 1994; De Backer et al., 2011) and neutral effects (de Deckere et al., 2000) on sediment resuspension have been observed depending upon the density of burrows and the sediment granulometry.

- Intermediate/deep-burrowing Polychaeta, that build complex gallery networks that can extend down to 30 cm depth, represented by *Hediste diversicolor* (Müller, 1776). This species may reach very high individuals densities (up to 5000  $Ind. m^{-2}$ ), especially in association with high organic load (Rasmussen, 1973; Abrantes et al., 1999). *H. diversicolor* are omnivores and detritivores that feed by swallowing surface sediments around the burrow opening. The burying depth is positively related to body length, although individuals longer than 10 cm can be commonly found in the upper 2–3 cm (Fernandes et al., 2006). *H. diversicolor* are known to create extensive gallery networks that they actively ventilate, increasing the flux of oxygen and nutrients over the sediment–water interface (Kristensen, 1983; Kristensen, 2001; Hedman et al., 2011; Zhu et al., 2016). The movements of *H. diversicolor* in the gallery network generate particles mixing in the surficial sediment layers and an accumulation of particles in the bottom layers due to non-local transport (Duport et al., 2006; Hedman et al., 2011). This species is considered by some authors as a stabiliser because it enhances stability by lateral compaction of the sediment around the burrows (Meadows and Tait, 1989; Meadows et al., 1990) and damp the hydrodynamic stress by the creation of skimming flow by protruding galleries (Friedrichs, 2011). Other authors have instead highlighted that *H. diversicolor*, while being able to increase the sediment resistance to initial motion, have a positive effect on sediment resuspension when the hydrodynamic stress increases (Fernandes et al., 2006).
- Deep-burrowing Polychaeta that live generally >10 cm deep in the sediment in J-shaped burrows, represented by *Arenicola marina* (Linnaeus, 1758). *A. marina* are large worms (up to 2 g AFDW) that swallow surface sediment through a feeding funnel and expel it in the form of pseudo-faeces, forming characteristic feeding pits and pseudo-faeces casts, (Zebe and Schiedek, 1996; Volkenborn et al., 2009). They are typically found in North European intertidal flats in densities of up to 100 individuals  $m^{-2}$  (Beukema and de Vlas, 1979). The sediment reworking from *A. marina* feeding activity increases the sediment volume exposed to hydrodynamic forcing and dramatically increase the resuspension of fine particles (Volkenborn et al., 2009; Wendelboe et al., 2013).

Considering the large number of flume runs needed, the time-consuming character of each flume experiment and the fact the bioturbators may exhibit seasonal variation in their behaviour, the experiments were performed during spring in two consecutive springs. Animals were collected between April–June 2011 and between April–June 2012 from the intertidal flats of the Oosterschelde and Westerschelde. The species involved in this study are not endangered or protected. The authorization for specimen collection was issued by the competent authority Rijkswaterstaat. The mortality during experiment was generally very low and the animals were released at the collection site at the end of the experiments.

To avoid confounding effect related to temperature variation, all experiments were performed at a constant temperature of 18 °C, i.e. the average water temperature in the Westerschelde and Oosterschelde during full summer. We chose this temperature because, due to the positive relationship between ectotherms' metabolic rates and temperature (Pörtner and Farrell, 2008), it is the one at which bioturbators should be



more active within their natural temperature range. At the time of collection, average daily water temperature was between 14 and 17 °C. After collection, the bioturbators were always allowed to acclimate for 1 week in containers filled with sediment and aerated filtered marine water that was kept at 18 °C. Considering the relatively limited difference in temperature between field and mesocosms, one week of acclimation (rather than the two weeks usually adopted in macrozoobenthos studies) should be sufficient to reduce the risk of temperature shock that could severely affect bioturbator metabolic rates (Nascimento et al., 1996). During the acclimation period the bioturbators have been fed with liquid algal extract or fish food. Experiments were performed directly after this week of acclimation.

Bioturbators' individual body mass (mg Ash Free Dry Weight, AFDW) was estimated from the individual length (mm, bivalves) or wet weight (mg, *A. marina*, *H. diversicolor*, *C. volutator*), according to the relationships provided from the NIOZ – Yerseke Monitor Taskforce. Bioturbators' individual metabolic rates were estimated according to the empirical model for aquatic macroinvertebrates respiration of Brey (2010) assuming an average energy density of 21.5 J mg<sup>-1</sup> (Brey, 2001) and an operational temperature of 18 °C and using a trait classification for sessile (bivalves, *A. marina*) or motile (*C. volutator* and *H. diversicolor*) intertidal satiate Annelida, Arthropoda or Bivalvia Heterodonta. The overall bioturbators population metabolic rate ( $I_{TOT}$ , mW m<sup>-2</sup>) was estimated as the product of the individual metabolic rate and the population density (Allen et al., 2005).

### 2.3. Experimental devices

The recirculating annular flumes we used follow the design described by (Widdows et al., 1998; Cozzoli et al., 2018a). The annular channel has a surface of 157 cm<sup>2</sup>. In the majority of the cases, we used flumes with an overall height of 40 cm, of which the bottom 5 cm are filled with a pebbled bed to allow water drainage, followed by 10 cm of consolidated sediment and 20 cm of filtered marine seawater (31.4 L). A modified version with an overall height of 80 cm and a sediment column of 50 cm was used to allow the largest sized *A. marina* to settle properly.

The muddy sediment used in this experiment (median grain size 120 μm, silt content 12% measured by using a Malvern Mastersizer 2000® particle analyser) was collected in late winter 2011 at location Zandkreek Dam (51°32'N, 3°52'E) in the Oosterschelde. The sediment was carefully sieved over a 1 mm sieve to avoid the presence of large particles (stones, shells, wooden pieces) and to remove large macrozoobenthos. It was then covered with a thick black plastic film for at least two weeks to kill remaining benthos and sieved again. As such, all macrozoobenthos was removed from the sediment. One week before of the experiments, the wet sediment was aerated and put in a flume, mixed to a smooth mass and allowed to consolidate. Although shorter than the time the sediment takes to return to a realistic porewater gradient after a big disturbance [13days according to Porter et al., 2006 (Porter et al., 2006)], preliminary observations showed that a one week consolidation time is sufficient to obtain a firm and homogeneous bottom between treatments.

The water motion in the annular flumes was generated by a smooth disk rotating 3 cm below the water surface, which was driven by a microprocessor-controlled engine. An acoustic Doppler velocimetry probe was used to calibrate water flow velocity as a function of engine rotation speed. The hydrodynamic Bed Shear Stress (BSS, Pa) was estimated from the depth-average water flow velocity  $v$  (m s<sup>-1</sup>) as:

$$BSS = \rho f v^2 \quad (1)$$

where  $\rho$  is the density of marine water (1024 kg m<sup>-3</sup>) and  $f$  is a constant friction factor, i.e. 0.002 (Roberts et al., 2000). We deliberately assign a constant  $f$  to exclude from Eq. (1) the possible influence of bioturbations on sediment surface friction. The friction of disrupted sediment surface

will thus be considered as property of the specimens and included in the bioturbation effect.

Water turbidity, as a proxy of suspended sediment, is measured using an optical backscatter sensor (OBS 3+, Campbell scientific) facing the water perpendicularly to the current direction at 10 cm from the sediment surface and measuring the water turbidity every 30 s. The effect of the suspended sediment on light absorption was measured by the OBS sensors and converted into Suspended Sediment Concentration (SSC, g L<sup>-1</sup>) based on calibration by gravimetric analysis (Cozzoli et al., 2018a). The SSC in the water is coupled with the mass of bottom sediment by a dynamic balance between deposition and erosion. Increasing bottom shear stress has the effect to increase the sediment erosion and decrease the sediment deposition, thus increasing the SSC. Analogously to previous studies [e.g. (Willows et al., 1998; van Prooijen et al., 2011)], we did not measure sediment deposition and we only consider the effect of bioturbation on the equilibrium SSC reached at a given level of bed shear stress from water motion (i.e., deposition rate = erosion rate, so that the suspended sediment concentration is constant). Previous studies (Willows et al., 1998; Ciutat et al., 2007; Li et al., 2017) have shown that, for this kind of experiment, supply-limited erosion mostly occurs. That is, after the water motion has started, the SSC reaches equilibrium due to limitation of erodible material (Mehta and Partheniades, 1982; van Prooijen and Winterwerp, 2010). In our experiments, the equilibrium SSC was usually reached after ca. 5 min of applying current. To express sediment resuspension in spatial units, we converted the SSC to total mass of suspended sediment per unit of sediment surface present in the flume ( $R_{TOT}$ , g m<sup>-2</sup>).

### 2.4. Experimental procedures

To simulate the natural dynamic changes in current velocity during the flood tide on a shallow flat, we increased the current in the experimental flumes from 10 cm s<sup>-1</sup> (Bed Shear Stress of 0.05 Pa) to 30 cm s<sup>-1</sup> (BSS of 0.25 Pa) by steps of 5 cm s<sup>-1</sup>, each step lasting 20 min. To determine the mass of suspended sediment per unit of sediment surface ( $R_{TOT}$ , g m<sup>-2</sup>) at each step of current velocity, we considered the average of the measurement collected in the last 2.5 min of the step, when the supply-limited suspended sediment concentration was quasi-stable.

The bottom sediment was smoothed before each replicate by running the flume without any bioturbator inside. As a consequence of the limited erosion that occurred during this procedure, a uniform, <0.5 mm-thick layer of fine sediment was deposited on the sediment surface of each flume within a few hours from the end of the run. Pilot experiments conducted in flumes without fauna, involving several sequential daily runs, showed some small differences across flumes, but no increase in sediment resuspension compared to the smoothing procedure.

After smoothing the bottom, bioturbators were evenly distributed over the sediment surface and allowed to settle for 48 h. The choice of a longer time interval (48 h) compared with the typical interval between erosion stress peaks (typically 12 or 24 h in a tidal system) was necessary to give the animals the time to properly settle in the new environment and recover from manipulation stress. The vast majority of them were buried within a few minutes after being placed in the flume and non-burrowing individuals were replaced. During their presence in the flume, some bivalves (especially *C. edule*) crawled on and below the sediment surface, leaving evident tracks. The intermediate burrowers bivalves left evident siphoning tracks around their burying site. Few *C. volutator* were swimming or crawling over the surface at a time, while the large majority was buried. *H. diversicolor* released mucus and faeces on the sediment surface while burying themselves and developed a system of galleries from which they rarely fully emerged. *A. marina* generally did not move from the initial settlement

point and produced a single feeding pit with a pseudo-faeces cast for each individual.

### 2.5. Data analysis

Assuming supply-limited sediment erosion (Mehta and Partheniades, 1982; van Prooijen and Winterwerp, 2010), the relationship between the mass of suspended sediment per unit of sediment surface ( $R_{TOT}$ ,  $g\ m^{-2}$ ) reached at each current velocity step and the applied hydrodynamic Bed Shear Stress (BSS, Pa) was modelled as a logistic sigmoidal curve:

$$R_{TOT} = \frac{a}{1 + e^{\frac{b-BSS}{c}}} \quad (2)$$

where the coefficient  $a$  is the maximal expected value of  $R_{TOT}$  (asymptote of the erosion curve,  $g\ m^{-2}$ ), the coefficient  $b$  is the BSS value at which 50% of the value of  $a$  is reached (midterm of the erosion curve, Pa) and  $c$  is a scale coefficient that allows accounting for the steepness of the curve at the inflection point. By analysing the data via non-linear mixed modelling (Bolker et al., 2009; Zuur et al., 2009), we allowed for random variations in the coefficients  $a$  and  $b$  across the full combination of bioturbators species, density and size gradients (Table 1).

Systematic variations in the asymptote  $a$  and the midterm  $b$  across the different treatments were analysed via linear ANCOVA. A multivariate regression model of each of the coefficients  $a$  and  $b$  was fitted using the bioturbators species as categorical variable and four basic descriptors of the investigated population as continuous variables: individual size ( $M$ , mg AFDW), density of individuals ( $D$ , N of Ind.  $m^{-2}$ ), total biomass ( $M_{TOT}$  mg AFDW  $m^{-2}$ ) and overall population metabolic rate ( $I_{TOT}$ ,  $mW\ m^{-2}$ ). To match the linear ANCOVA assumptions, the asymptote  $a$  distribution was normalized via log transformation and the distribution of the variables individual size, density of individuals, total biomass and  $I_{TOT}$  was normalized via log plus 1 transformation. The best predictors were selected by AIC comparison and elimination stepwise procedure. The relative importance of the predictors in explaining variance was assessed by LMG metrics [ $R^2$  partitioned by averaging over orders (Lindeman et al., 1980)]. All analyses were performed within the free software environment R 3.3.2 (R-Core-Team, 2017) using the lmer (Bates et al., 2015) and relaimpo (Grömping, 2006) packages.

### 3. Results

All the tests show that mass of suspended sediment per unit of sediment surface ( $R_{TOT}$ ,  $g\ m^{-2}$ ) increases consistently with the Bed Shear Stress (BSS, Pa). The highest  $R_{TOT}$  recorded in the defaunated controls was  $40.02\ g\ m^{-2}$  at the maximal BSS of 0.25 Pa. Values of  $R_{TOT}$  higher than  $150\ g\ m^{-2}$  were recorded in presence of bioturbators due to general failures of the flume bed and consequent mass erosion. These values were not accounted for in the analysis. After this skimming, the highest recorded  $R_{TOT}$  was  $133\ g\ m^{-2}$  for *S. plana* (large individuals) at BSS of 0.18 Pa. A slight decrease in  $R_{TOT}$  was observed at low BSS and low densities of bioturbators (Fig. 1). Exceptional behaviour was shown by *H. diversicolor*, which are able to considerably decrease  $R_{TOT}$  up to a BSS of 0.20 Pa at each tested density of individuals.

A logistic sigmoidal function of the BSS (Eq. (2)) was able to explain 53% of the marginal variance of  $R_{TOT}$  (i.e. that part of variance of  $R_{TOT}$  attributable to the fixed factor BSS) Accounting for random variations in the asymptote  $a$  and the midterm  $b$  for each treatment, 97% of the conditional variance of  $R_{TOT}$  (i.e. that part of variance of  $R_{TOT}$  attributable to both the fixed factor BSS and the random variation across treatments) was explained (Fig. 1, Table 2).

The presence of bioturbators has the effect to increase both the maximal (asymptotic) amount of eroded sediment (coefficient  $a$  in Eq. (2)) and the hydrodynamic energy needed to reach the midterm of the erosion curve (coefficient  $b$  in Eq. (2)) (Table 1).

As a single descriptor, the overall population metabolic rate of the bioturbators ( $I_{TOT}$ ,  $mW\ m^{-2}$ ) is able to explain most of the variance (54%) in the asymptote  $a$  (Table 3) with better performance than the other descriptors considered (i.e. Individual Size, Density of Individuals and overall Biomass; Appendix B, Table B1) [ $\pm 95\%$  CI]:

$$a_{BIO} = 40.45[\pm 9.95] * (1 + I_{TOT})^{0.24[\pm 0.07]} \quad (3.1)$$

In association with other descriptors, the individual size of the bioturbators ( $M$ , mg AFDW) have also been selected via stepwise procedure as significant explanatory variable. The negative relationship with  $M$  contributes to explain a further 8% of variance in  $a_{BIO}$  (Table 3):

$$a_{BIO} = 41.67[\pm 9.07] * (1 + I_{TOT})^{0.34[\pm 0.12]} * (1 + M)^{-0.09[\pm 0.06]} \quad (3.2)$$

The stepwise variable selection excludes significant interspecific variations of  $a_{BIO}$  (Table 3).

$I_{TOT}$  is also a significant descriptor of the midterm  $b$  of the erosion curve, despite being able to explain a smaller amount of variance (20%) than it does for the asymptote  $a_{BIO}$  (Table 4):

$$b_{BIO} = 0.1[\pm 0.04] + 0.02[\pm 0.01] * \log(1 + I_{TOT}) \quad (4.1)$$

As a single population descriptor, the metabolic rate has a performance comparable to the total biomass and higher than that of the individual size or density of individuals in describing the variance of  $b_{BIO}$  (Appendix B, Table B2). Differently from the asymptote  $a_{BIO}$ , the midterm  $b_{BIO}$  is subject to significant interspecific variations, to which 50% of the observed variance can be attributed (Table 4):

$$b_{BIO} = 0.1[\pm 0.03] + 0.01[\pm 0.009] * \log(1 + I_{TOT}) + Species \quad (4.2)$$

The interspecific variability of  $b_{BIO}$  is mostly related to the effect of *H. diversicolor*, the only species for which we observed a strongly significant ( $p < 0.001$ ) higher  $b$  value than for other species (Tables 1, 4).

In all cases, the intercepts of the scaling models (i.e. condition of absence of bioturbators) match the values of  $a$  and  $b$  estimated for defaunated controls, indicating that the models are compatible with a physical description of the relationship between BSS and cohesive sediment resuspension (Tables 3, 4).

From Eqs. (3.1) and (4.1) it follows that  $R_{TOT}$  may be predicted as a function of the combination of BSS and  $I_{TOT}$  by replacing in Eq. (2) the parameter  $a$  by  $a_{BIO}$  and replacing  $b$  by  $b_{BIO}$  (Fig. 2):

$$R_{TOT} = \frac{a_{BIO}}{1 + e^{\frac{b_{BIO}-BSS}{c}}} \quad (5)$$

Eq. (5) is able to explain 62% of the variance in the observed  $R_{TOT}$  values, with a ratio between observed and predicted values very close to 1:1 (Fig. 3, Table 5). Including the negative dependence of  $a_{BIO}$  from the individual size (Eq. (3.2)), the variance in the observed  $R_{TOT}$  values explained by Eq. (5) rises to 64% and reaches 78% if the interspecific variations of the midterm (Eq. (4.2)) are considered (Fig. 3, Table 5). This means that a heterogeneous process such as sediment resuspension induced by bioturbators with different functional characteristics can be effectively described as a function of  $I_{TOT}$  and BSS, accounting for some differences for bioturbators species with different functional characteristics as *H. diversicolor*.

### 4. Discussion

In this paper, we derive a unified view of bioturbation effects on supply-limited resuspension of cohesive sediment and a general relationship to quantify such effect along a hydrodynamic stress gradient (Eq. (5)). Eq. (5) provides a description of a physical trend (relationship between Bed Shear Stress and cohesive sediment supply-limited

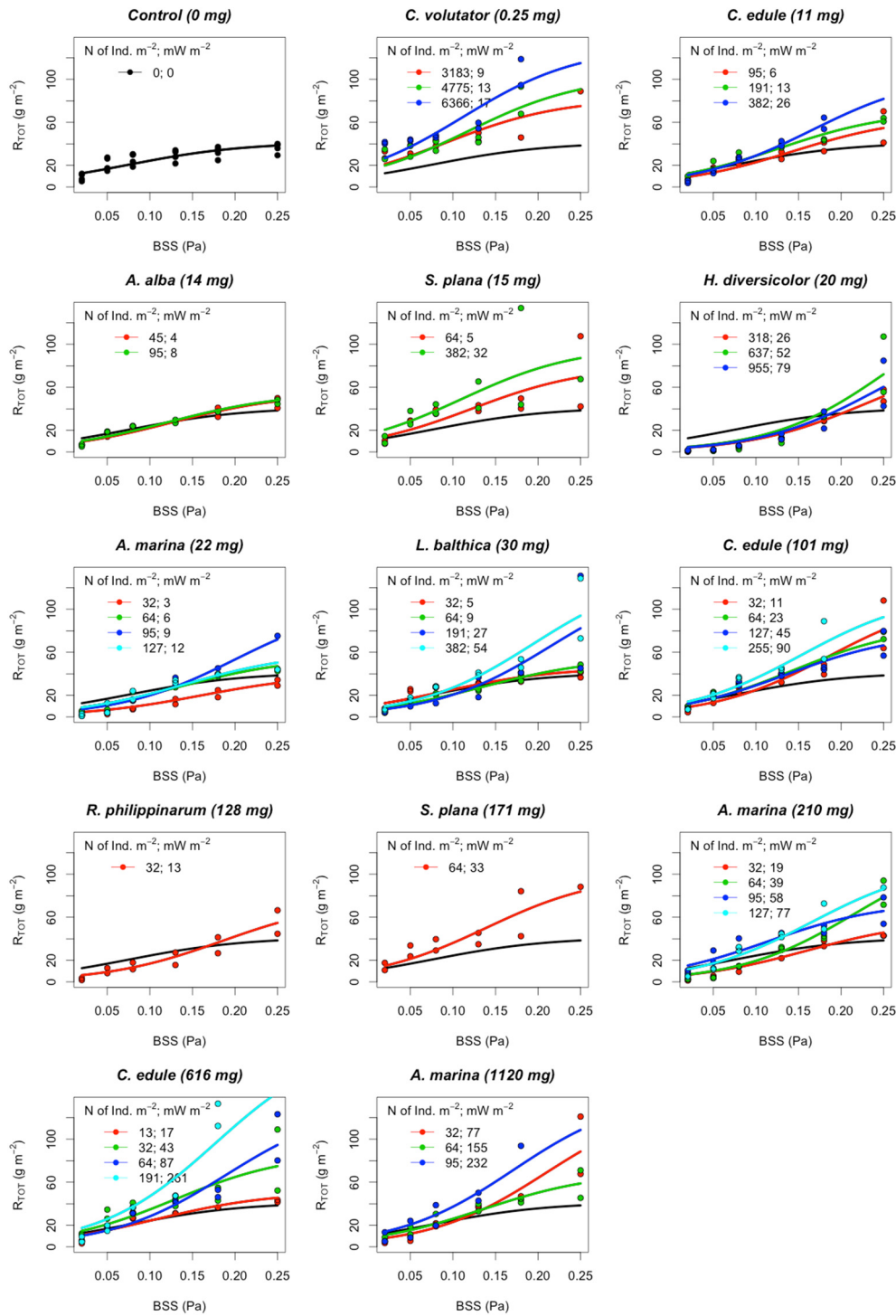


**Fig. 1.** Relationship between  $R_{TOT}$  (total mass of suspended sediment,  $\text{g m}^{-2}$ ) and Bed Shear Stress (BSS, Pa) for different species, individual sizes and densities of bioturbators (coloured lines), ordered by the individual size of the bioturbators. The black line shows the defaunated control. The relationship was modelled as a logistic sigmoidal curve  $R_{TOT} = a / (1 + e^{(b - \text{BSS})/c})$  allowing random variations in the asymptote  $a$  and midpoint  $b$  for each treatment (Table 2).

erosion, shaped as a sigmoidal curve) in which the physical constants (the asymptote  $a$  and the midterm  $b$ ) are replaced by empirical descriptions of the behaviour of organisms ( $a_{BIO}$  and  $b_{BIO}$ , Fig. 2). It meets the requirements indicated by van Prooijen, et al. (van Prooijen et al., 2011) for process-based models of bio-mediated physical dynamics in the sense that: *i*) it is composed of a set of formulations representing sub-processes (*i.e.* the physical effect of Bed Shear Stress on cohesive sediment resuspension; the effect of bioturbators on the amount of sediment suspended at different BSS) *ii*) it is mainly based on general

ecological principles of size and energy scaling that should hold for any organism, although with some specific variation in the parameters *iii*) it is fully compatible with a physical description of the processes in case of no biogenic influences, as the intercepts of the scaling models for the coefficients  $a_{BIO}$  and  $b_{BIO}$  match the values predicted for the defaunated control; *iv*) it is affected by a minimum number of physically well-defined parameters (mainly BSS and energy use rate of the bioturbators, in this study case). Being a process based model, Eq. (5) has the potential to be further developed to include additional processes

**Table 2**

Summary of the mixed logistic model  $R_{TOT}$ -BSS. The relationship was modelled as a logistic curve  $R_{TOT} = a/1 + e^{(b-BSS)/c}$  allowing random variations in the asymptote  $a$  and midpoint  $b$  across the full factorial combinations of bioturbators species, densities and size gradients, while the scaling coefficient  $c$  was kept constant.

| Predictors                        | $R_{TOT} = a/1 + e^{(b-BSS)/c}$ |      |        |
|-----------------------------------|---------------------------------|------|--------|
|                                   | Est.                            | SE   | $p$    |
| $a$                               | 92.96                           | 4.81 | <0.001 |
| $b$                               | 0.16                            | 0.01 | <0.001 |
| $c$                               | 0.07                            | 0.00 | <0.001 |
| <b>Random effects</b>             |                                 |      |        |
| $\sigma^2$                        | 103.27                          |      |        |
| $\tau_{00}$ Treatment             | 1614.69                         |      |        |
| $\tau_{11}$ Treatment <b>b</b>    | 0.00                            |      |        |
| $\rho_{01}$ Treatment             | 0.54                            |      |        |
| ICC <sub>Treatment</sub>          | 0.94                            |      |        |
| Observations                      | 460                             |      |        |
| Marginal $R^2$ /conditional $R^2$ | 0.527/0.972                     |      |        |

generating variance in  $a_{BIO}$  and  $b_{BIO}$  (e.g. different typologies of sediment, different typologies of ecosystem engineers). It must be however considered that, in its present form, Eq. (5) concerns supply-limited erosion only (Mehta and Partheniades, 1982; van Prooijen and Winterwerp, 2010). At a BSS higher than the maximal we tested, mass erosion may overcome the importance of bioturbation in determining sediment resuspension.

Within the range of tested conditions, random variations across treatments with different bioturbator species, size and density were as important as the fixed effect of hydraulic Bed Shear Stress (BSS) in explaining variations in the mass of suspended sediment. Different population descriptors such as the individual size, the density of individuals or the total biomass may be used as proxy for the bioturbators effect on sediment resuspension. The metabolic rate is a more general index which encompasses these multiple parameters, and it has the advantage of being mechanistically related to the organisms' bioturbation activity, rather than being a proxy of it. Variations in  $a_{BIO}$  and  $b_{BIO}$  can be efficiently described in terms of overall bioturbators population metabolic rate, although descriptions of the individual size ( $a_{BIO}$ ) and species-specificities ( $b_{BIO}$ ) of bioturbators may contribute in improving the accuracy of Eq. (5).

**Table 3**

Summary of the linear ANCOVA model of the asymptote of the logistic erosion curve ( $a_{BIO}$ ) fitted using the bioturbators species as categorical variable and four basic descriptors of the investigated population as continuous variables: individual size ( $M$ , mg AFDW), density of individuals ( $D$ , N of Ind.  $m^{-2}$ ), total biomass ( $M_{TOT}$  mg AFDW  $m^{-2}$ ) and overall population metabolic rate ( $I_{TOT}$ ,  $mW m^{-2}$ ). The asymptote  $a_{BIO}$  was log transformed and the continuous explanatory variables were log plus 1 transformed. The table shows the estimates parameters (Est., expressed as difference from the Control value) with associated standard error (SE) and significance value ( $p$ ). The left column shows the full model. The central column shows the best fitted model as selected by stepwise elimination procedure. The right column show the model fitted  $I_{TOT}$  as the only predictor.

| Predictors              | Full        |      |        | log(1 + M) + log(1 + I <sub>TOT</sub> ) |      |        | log(1 + I <sub>TOT</sub> ) |      |        |
|-------------------------|-------------|------|--------|---|------|--------|----------------------------|------|--------|
|                         | Est.        | SE   | $p$    | Est.                                    | SE   | $p$    | Est.                       | SE   | $p$    |
| Intercept (control)     | 3.72        | 0.26 | <0.001 | 3.73                                    | 0.11 | <0.001 | 3.70                       | 0.12 | <0.001 |
| $M$                     | -2.05       | 3.57 | 0.57   | -0.09                                   | 0.03 | <0.001 |                            |      |        |
| $D$                     | -1.88       | 3.64 | 0.61   |   |      |        |                            |      |        |
| $M_{TOT}$               | 2.21        | 3.32 | 0.51   |   |      |        |                            |      |        |
| $I_{TOT}$               | -0.03       | 0.84 | 0.97   | 0.34                                    | 0.04 | <0.001 | 0.24                       | 0.04 | <0.001 |
| <i>A. alba</i>          | -1.29       | 3.84 | 0.74   |   |      |        |                            |      |        |
| <i>A. marina</i>        | -5.67       | 6.31 | 0.38   |   |      |        |                            |      |        |
| <i>C. edule</i>         | -1.21       | 3.95 | 0.76   |   |      |        |                            |      |        |
| <i>C. volutator</i>     | 1.72        | 8.34 | 0.84   |   |      |        |                            |      |        |
| <i>M. balthica</i>      | -1.24       | 3.87 | 0.75   |   |      |        |                            |      |        |
| <i>H. diversicolor</i>  | -8.45       | 9.98 | 0.40   |   |      |        |                            |      |        |
| <i>S. plana</i>         | -1.12       | 3.91 | 0.78   |   |      |        |                            |      |        |
| <i>R. philippinarum</i> | -1.16       | 3.93 | 0.77   |   |      |        |                            |      |        |
| Observations            | 39          |      |        | 39                                      |      |        | 39                         |      |        |
| $R^2$ /adj $R^2$        | 0.687/0.542 |      |        | 0.654/0.635                             |      |        | 0.544/0.531                |      |        |
| AIC                     | 19.183      |      |        | 3.030                                   |      |        | 11.841                     |      |        |

**Table 4**

Summary of the linear ANCOVA model of the midterm of the logistic erosion curve ( $b_{BIO}$ ) fitted using the bioturbators species as categorical variable and four basic descriptors of the investigated population as continuous variables: individual size ( $M$ , mg AFDW), density of individuals ( $D$ , N of Ind.  $m^{-2}$ ), total biomass ( $M_{TOT}$  mg AFDW  $m^{-2}$ ) and overall population metabolic rate ( $I_{TOT}$ ,  $mW m^{-2}$ ). The continuous explanatory variables were log plus 1 transformed. The table shows the estimates parameters (Est., expressed as difference from the Control value) with associated standard error (SE) and significance value ( $p$ ). The left column shows the full model. The central column shows the best fitted model as selected by stepwise elimination procedure. The right column show the model fitted using  $I_{TOT}$  as the only predictor.

| Predictors              | Full        |      |      | log(1 + I <sub>TOT</sub> ) + species |      |        | log(1 + I <sub>TOT</sub> ) |      |        |
|-------------------------|-------------|------|------|--------------------------------------|------|--------|----------------------------|------|--------|
|                         | Est.        | SE   | $p$  | Est.                                 | SE   | $p$    | Est.                       | SE   | $p$    |
| Intercept (control)     | 0.08        | 0.03 | 0.02 | 0.08                                 | 0.03 | 0.02   | 0.1                        | 0.02 | <0.001 |
| $M$                     | -0.19       | 0.42 | 0.65 |                                      |      |        |                            |      |        |
| $D$                     | -0.18       | 0.43 | 0.68 |                                      |      |        |                            |      |        |
| $M_{TOT}$               | 0.22        | 0.39 | 0.58 |                                      |      |        |                            |      |        |
| $I_{TOT}$               | -0.03       | 0.10 | 0.75 | 0.01                                 | 0.01 | 0.09   | 0.02                       | 0.01 | <0.001 |
| <i>A. alba</i>          | -0.12       | 0.45 | 0.79 | 0.03                                 | 0.04 | 0.42   |                            |      |        |
| <i>A. marina</i>        | -0.53       | 0.74 | 0.48 | 0.06                                 | 0.04 | 0.12   |                            |      |        |
| <i>C. edule</i>         | -0.11       | 0.46 | 0.81 | 0.04                                 | 0.04 | 0.24   |                            |      |        |
| <i>C. volutator</i>     | 0.11        | 0.98 | 0.91 | 0.01                                 | 0.04 | 0.82   |                            |      |        |
| <i>M. balthica</i>      | -0.11       | 0.45 | 0.82 | 0.06                                 | 0.04 | 0.14   |                            |      |        |
| <i>H. diversicolor</i>  | -0.75       | 1.17 | 0.53 | 0.13                                 | 0.04 | <0.001 |                            |      |        |
| <i>S. plana</i>         | -0.14       | 0.46 | 0.77 | 0.02                                 | 0.04 | 0.57   |                            |      |        |
| <i>R. philippinarum</i> | -0.07       | 0.46 | 0.88 | 0.09                                 | 0.04 | 0.07   |                            |      |        |
| Observations            | 39          |      |      | 39                                   |      |        | 39                         |      |        |
| $R^2$ /adj $R^2$        | 0.649/0.487 |      |      | 0.631/0.517                          |      |        | 0.226/0.205                |      |        |
| AIC                     | -148.006    |      |      | -152.028                             |      |        | -139.32                    |      |        |

4.1. Effect of bioturbator metabolism on the amount of suspended sediment at high BSS

The most important biological driver for amount of destabilized and suspended sediment at high BSS is the overall bioturbators population metabolic rate, which explains 56% of the cross-treatment variation in the asymptote of the erosion curve (coefficient  $a_{BIO}$  in Eq. (5)). This is related to the fact that the bioturbators' activities are able to disrupt cohesiveness and compaction in the upper layers of sediment, generating a fluff layer that starts to be suspended from a BSS of ca. 0.15 Pa (Orvain et al., 2003; van Prooijen et al., 2011). Our measurements show that the overall amount of sediment contained in the fluff layer is proportional to



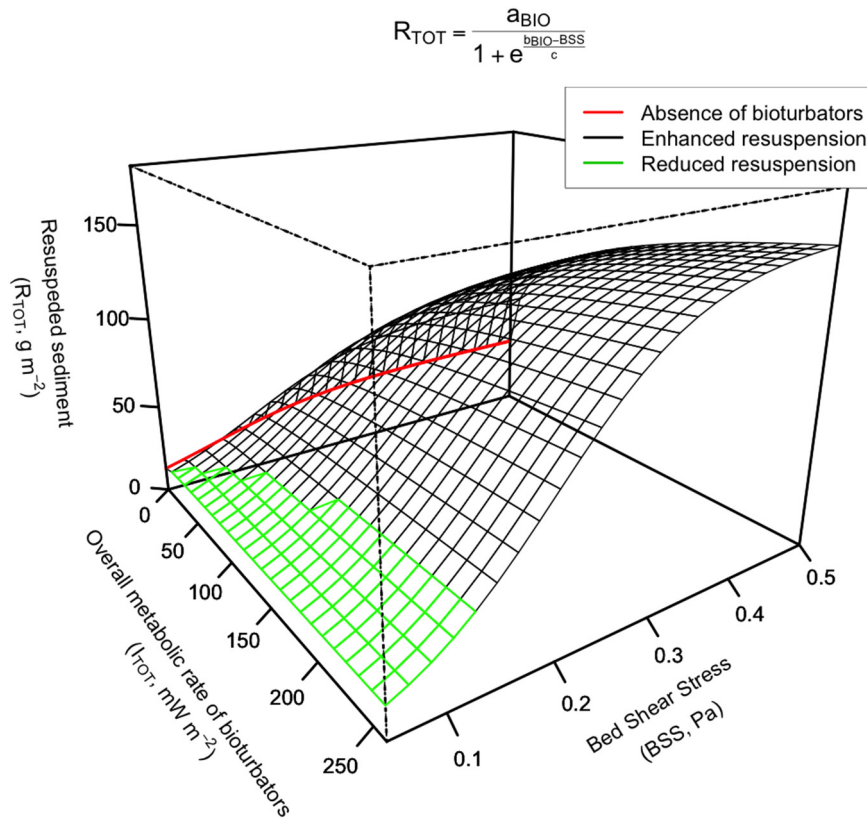


**Fig. 2.** Relationship between amount of suspended sediment ( $R_{TOT}$ ,  $g\ m^{-2}$ ), metabolic rate of the bioturbating population ( $I_{TOT}$ ,  $mW\ m^{-2}$ ) and Bed Shear Stress (BSS, Pa). The relationship was modelled as a logistic sigmoidal curve  $R_{TOT} = a_{BIO} / (1 + e^{(b_{BIO} - BSS)/c})$ , accounting for the variation of the asymptote  $a_{BIO}$  ( $g\ m^{-2}$ ) and the midterm  $b_{BIO}$  (Pa) at the variation of  $I_{TOT}$  as predicted from Eqs. (3.1) and (4.1). The red line shows the defaunated control. The green part of the grid shows the conditions in which the bioturbators reduce the sediment resuspension.

the activity (approximated as population basal metabolic rate) of the bioturbators inhabiting the sediment.

A minor but significant variant component of the coefficient  $a_{BIO}$  (8%) is explained by a negative relationship with individual body size. A potential interpretation for this trend is that smaller individuals dig less deeply (Zwarts and Wanink, 1989; Zebe and Schiedek, 1996; Fernandes et al., 2006), causing them to use their energy to rework more surficial and exposed sediment. It is also possible that smaller individuals could represent earlier life stages, characterized by higher metabolic rates (Glazier, 2005; Glazier et al., 2011) than what we have estimated from the empirical model of Brey (2010).

#### 4.2. Effect of bioturbators metabolism on the amount of suspended sediment at low BSS

The presence of bioturbators has the effect to increase the hydrodynamic energy needed to reach the midterm of the erosion logistic curve ( $b_{BIO}$  in Eq. (5)). Species-specific differences have a major importance in determining the value of  $b_{BIO}$ . Together with specific variations, we observed a positive relationship between  $b_{BIO}$  and the overall bioturbators population metabolic rate. This indicates that at high levels of bioturbation activity, a proportionally lower amount of sediment is suspended at low BSS. This pattern is possibly related to the fact that bioturbators are able to shelter the sediment surface from shear flow when the hydrodynamic forcing is low (Friedrichs et al., 2009; Friedrichs, 2011). The reworking by the animals could also change the structure of the sediment: excreted sediments can be pelletized and compacted, becoming slightly more resistant to initial erosion (Briggs et al., 2015). The positive dependence of the midterm  $b_{BIO}$  on population metabolism may be explained by considering that these processes (changes in microtopography of the sediment surface, pelletization of the sediment)

are also products of the bioturbators' activity and metabolism, hence they should scale positively with the individual size and density of individuals. However, bioturbation led only to a minor reduction in suspended sediment at low BSS, that is suppressed at higher BSS by the opposite destabilizing effect.

#### 4.3. Effect of different types of bioturbators

We observed that differences in bioturbators species and functional behaviour do not have a significant influence on the (asymptotic) amount of sediment suspended at high BSS ( $a_{BIO}$ ), implying that all of these species ultimately move the same maximal amount of sediment per unit of metabolic rate. Instead, the midterm of the erosion logistic curve ( $b_{BIO}$ ) varies across species, mostly in relation to the effect of the gallery-builder *H. diversicolor*. Compared to other species, *H. diversicolor* markedly reduce sediment resuspension at low BSS (<0.2 Pa). This observation could represent a stabilizing effect of this species, that is likely related to the lateral compaction of the gallery walls during burrowing activity and to the secretion of mucus that is pushed against the walls, both consolidating the burrows and increasing the cohesiveness of the sediment (Meadows and Tait, 1989; Meadows et al., 1990; Fernandes et al., 2006). Considering that *H. diversicolor* also displaces surface particles down to the gallery bottom (Duport et al., 2006; Hedman et al., 2011), dissolve the internal pool of particulate nutrients in the sediment (Ieno et al., 2006; Hedman et al., 2011) and contribute to seed burial (Zhu et al., 2016) it is possible that this species, at BSS and individual densities comparable to what we tested, may promote the compaction of the recently deposited sediment and the accretion of tidal flats and marshes. However, the sediment stabilizing effect of *H. diversicolor* is limited to low shear stress. When the BSS reaches and exceeds 0.20 Pa, *H. diversicolor* have an effect similar to the other bioturbators, confirming

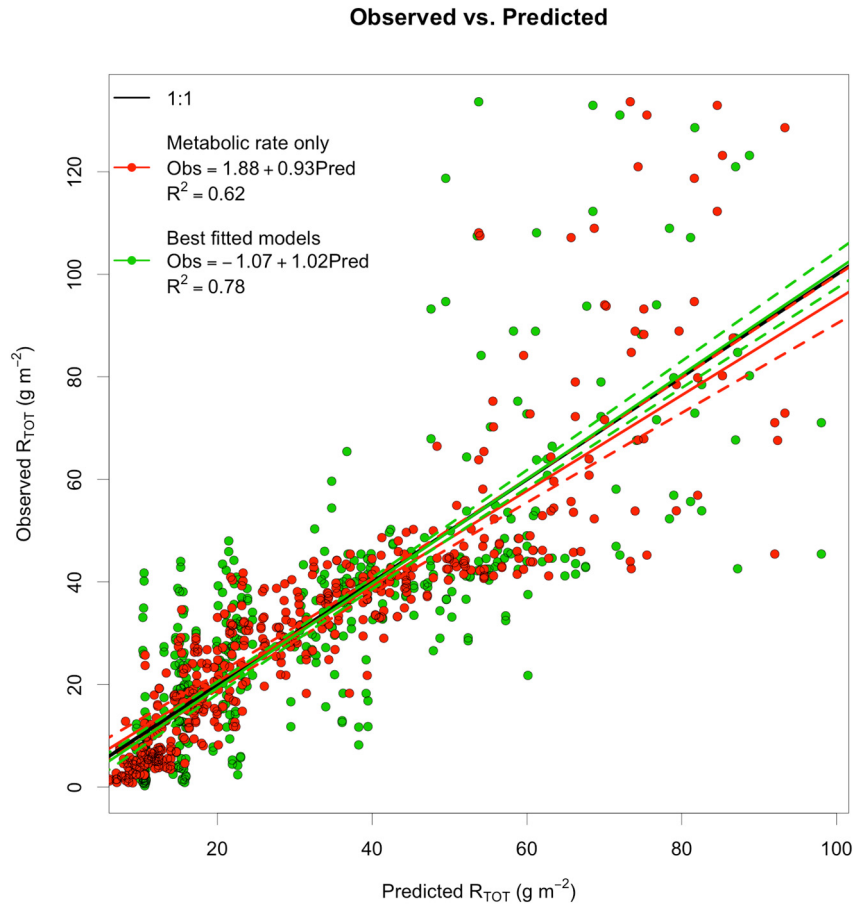


**Fig. 3.** Relationship between observed sediment resuspension in our experiments ( $R_{TOT} \text{ g m}^{-2}$ ) and predictions from Eq. (5):  $R_{TOT} = a_{BIO}/1 + e^{(b - BSS)/c}$ . The black full line show the 1:1 ratio. Full coloured lines show the average trend; dashed lines show the 95% Confidence Interval around the average trend. The red points and lines show the prediction of Eq. (5) using the metabolic rate of the bioturbations population as only descriptor for variations in  $a_{BIO}$  and  $b_{BIO}$ . The green points and lines show the prediction of Eq. (5) including also the negative dependence of  $a_{BIO}$  from the individual size and allowing interspecific variations in  $b_{BIO}$  (Table 5).

what was earlier reported by previous studies (Fernandes et al., 2006; Widdows et al., 2009). Also, at higher densities of individuals ( $3000 \text{ Ind. m}^{-2}$ ) than what we tested in our experiments ( $318\text{--}955 \text{ Ind. m}^{-2}$ ) *H. diversicolor* have been observed to increase sediment resuspension even at low hydrodynamic stress (Widdows et al., 2009).

Our measurements were focused on single species and homogeneous size experiments in order to emphasize scaling relationships. The effects of individual species on sediment resuspension in a mixed benthic community may be rather complex, depending on how interspecific interactions affect the activity of the involved species; these must also be accounted for in order to extrapolate mesocosm

observations to field contexts (Orvain et al., 2012; Kristensen et al., 2013). A particularly important interaction to be accounted for in field conditions is that one with biostabilizers (i.e. organisms that are able to enhance the sediment resistance to erosion). As an example, the microphytobenthos, that is also abundant in the upper part of intertidal flats, can produce sticky extracellular polymeric substances (Vos et al., 1998) able to increase sediment resistance to erosion (Sutherland and Grant, 1998; Tolhurst et al., 2006). On the one hand, by disrupting and grazing the diatom film, benthic bioturbators may have a much higher relative impact on mudflat morphology than what we measured in our flumes because they are able to trigger the resuspension of sediment that is otherwise stabilised by diatoms (Montserrat et al., 2008) and therefore more resistant to erosion than our sediment controls free of phytobenthos. On the other hand, bioturbators may promote the microphytobenthos growth by organically enriching the sediment via biodeposition [i.e. (Andersen et al., 2010; Donadi et al., 2013)]. As another example, biostabilizers such as sessile tube-builder worms (e.g. *Lanice conchilega*), reef forming bivalves (e.g. mussels, oysters) and riparian plants (e.g. *Spartina anglica*, *Phragmites australis*) occur in dense reefs, tussocks or canopies that exclude bioturbators inside them. However, they can modify the hydrodynamics and the sedimentary landscape around their aggregates, affecting the conditions relevant to determine the bioturbators community size/density structure (Wallis et al., 2015). In turn, sediment destabilization and seed predation from bioturbators may affect the establishment of biostabilizers (van Wesenbeeck et al., 2007; Suykerbuyk et al., 2012; Zhu et al., 2016). The interplay between biostabilizers and biodestabilizers needs to be

**Table 5**

Linear relationship the observed values of  $R_{TOT}$  in the flume experiments and the prediction of the logistic model  $R_{TOT} = a/1 + e^{(b - BSS)/c}$ , accounting for the effect of metabolic rate only (left column, Eqs. (3.1) and (4.1)), including negative dependence of the asymptote  $a_{BIO}$  from the individual size (central column, Eqs. (3.2) and (4.1)) and species specific differences in the midterm  $b_{BIO}$  (right column, Eqs. (3.2) and (4.2)).

| Predictors            | Metabolic rate |      |        | Metabolic rate + individual size |      |        | Metabolic rate + individual size + species |      |        |
|-----------------------|----------------|------|--------|----------------------------------|------|--------|--|------|--------|
|                       | Est.           | SE   | p      | Est.                             | SE   | p      | Est.                                       | SE   | p      |
| Intercept             | 1.88           | 1.28 | 0.14   | 1.87                             | 1.24 | 0.13   | -1.07                                      | 0.98 | 0.28   |
| Predicted $R_{TOT}$   | 0.93           | 0.03 | <0.001 | 0.93                             | 0.03 | <0.001 | 1.02                                       | 0.03 | <0.001 |
| Observations          | 460            |      |        | 460                              |      |        | 460  |      |        |
| $R^2$ /adjusted $R^2$ | 0.626/0.625    |      |        | 0.642/0.641                      |      |        | 0.777/0.777                                |      |        |

taken into account for a more complete understanding of the biotic influences of sediment resuspension.

Being mostly based on general size scaling laws, Eq. (5) has the potential to be applied to describe the effect of a broader size and functional range of ecosystem engineers than what we tested in our experiment. As an example, it could be adapted to describe the effect of biodepositors (*i.e.* organisms that with their activity or presence establish a positive net flux of particles from the water column to the bottom, *e.g.* filtrators) and biostabilizers (*i.e.* organisms that with their activity and presence make the sediment more resistant to erosion) on sediment resuspension by allowing negative metabolic dependence of the asymptote  $a_{BIO}$  and stronger positive metabolic dependence of the midterm  $b_{BIO}$ . For organisms influencing the sediment dynamics mainly by their presence rather than activity, the overall biovolume may be a more appropriate descriptor of their effect on sediment resuspension than  $I_{TOT}$ .

#### 4.4. Application potential

Ecological theory that is grounded in metabolic currencies and constraints offers the potential to link ecological outcomes to biophysical processes across multiple scales of organization (Humphries and McCann, 2014). Descriptions of ecosystem engineering have a particular relevance in predicting changes in landscape evolution (Pearce, 2011). Process-based models of bioturbation effects such as those we presented may contribute to the prediction of both long and short-term morphodynamic trends (Hu et al., 2015; Hu et al., 2018) also as response to human modifications of coastal landscapes (Cozzoli et al., 2017; Valdemarsen et al., 2018). Having such a metabolism-based relationship does enable extrapolations on how change in benthic community metabolism may influence bioturbation effects on sediment resuspension.

Formulations describing the field distribution of bioturbators metabolic rates with respect to environmental conditions may be included in Eq. (5) as sub-processes. For local applications, the metabolic rate of bioturbator communities (and therefore their potential contribution to sediment resuspension) can be estimated with good approximation from field surveys, or they can be predicted by using empirical models relating average size and density of benthic communities to the environmental conditions in which they occur [*e.g.* (Cozzoli et al., 2017; Gjoni et al., 2017; Gjoni and Basset, 2018)], in association with empirical models of metabolic rates of benthic invertebrates [*e.g.* (Brey, 2010)]. About this point, it is important to consider that the hydrodynamic stress is a main driver of realized macrozoobenthic community composition and size structure [*e.g.* (Ysebaert and Herman, 2002; Thrush et al., 2005; Cozzoli et al., 2017)]. This implies that both the spatial distribution of bioturbators and the combined effect of hydrodynamic stress and bioturbators on sediment resuspension and can be fundamentally predicted by the same prognostic hydrodynamic model. Remote sensing of primary production [*e.g.* (Daggers et al., 2018)] and carbon fluxes [*e.g.* (Brock et al., 2006)] and models of energy flow across trophic levels [*e.g.* (van der Meer et al., 2013)] may be used to estimate the metabolic rate of benthic communities from satellite observations and therefore their impact on sediment resuspension.

Beyond size, metabolic rates of ectotherms are strongly dependent on the environmental temperature according to a positive Boltzmann-Arrhenius relationship (Clark and Johnston, 1999; Gillooly et al., 2001; Ernest et al., 2003; Gillooly et al., 2006; Clarck, 2006; Pörtner and Farrell, 2008). Accounting for the effect of temperature into metabolic – mediated sediment resuspension models may help explaining seasonal variations in biotic contribution to sediment transport (Cozzoli et al., 2018a; Wrede et al., 2018). To more broadly predict and compare the biotic contribution to sediment resuspension across different ecosystems, general allometric theories of scaling of metabolic rates with temperature, individual size and population density [*e.g.* (Damuth, 1991; Kooijman, 2000; Brown et al., 2004; Brown et al., 2007)] may be

joined to general models of benthic community structure in streams and transitional waters [*e.g.* (Vannote et al., 1980; Pearson and Rosenberg, 1978; Guelorget and Perthuisot, 1992; Tagliapietra et al., 2012)].

## 5. Conclusion

With this study, we developed a unified view and general approach to scale the effects of bioturbation on sediment erodibility along a hydrodynamic stress gradient. We showed that the effect of bioturbators on cohesive sediment resuspension can be described by bioturbators' population metabolic rate, with minor variations across different bioturbation modalities. This finding is in-line with other studies showing that indicators based on community size structure, rather than on species-specific characteristics, can be used to describe functional ecological processes or patterns such as community interactions (McGill et al., 2006) and structure (Gjoni et al., 2017; Gjoni and Basset, 2018), resource exploitation (Basset et al., 2012a; Cozzoli et al., 2018b; Cozzoli et al., 2019), species coexistence (Canavero et al., 2014), habitat carrying capacity (Edgar, 1993) and ecological status (Mouillot et al., 2006; Menezes et al., 2010; Basset et al., 2012b).

This is important as it allows to place empirical observations of biota-sediment interactions in the broader frame of general energetic theories [*e.g.* (Kooijman, 2000; Brown et al., 2004)], establishing a link between the metabolic rates of individuals and the ecological roles of organisms in geomorphology and landscape evolution.

### CRedit authorship contribution statement

**Francesco Cozzoli:** Conceptualization, Data curation, Formal analysis, Investigation, Methodology, Resources, Software, Visualization, Writing - original draft. **Vojsava Gjoni:** Writing - review & editing. **Michela Del Pasqua:** Writing - review & editing. **Zhan Hu:** Writing - review & editing. **Tom Ysebaert:** Conceptualization, Writing - review & editing. **Peter M.J. Herman:** Conceptualization, Writing - review & editing, Funding acquisition, Project administration. **Tjeerd J. Bouma:** Conceptualization, Writing - review & editing, Funding acquisition, Project administration.

### Acknowledgments

We gratefully thank the following people and companies: Conrad Pilditch for providing insights on the flumes realization; Jansen Tholen B.V. for the flumes realization, Lowie Haazen, Bert Sinke, Jos van Soelen for their fundamental technical support and for their patience; Nilawati, for her contribution during the experiments; three anonymous reviewers for their insightful comments that greatly contribute to the improvement of this paper. This work was funded by the Ecoshape/Building with Nature project, with the contribution of the CoE-Oesterdam project. At the time of starting this project, NIOZ-Yerseke belonged to the Netherlands Institute of Ecology.

### Appendices. Supplementary data

Supplementary data to this article can be found online at <https://doi.org/10.1016/j.scitotenv.2019.03.085>.

### References

- Abrantes, A., Pinto, F., Moreira, M., 1999. Ecology of the polychaete *Nereis diversicolor* in the Canal de Mira (Ria de Aveiro, Portugal): population dynamics, production and oogenic cycle. *Acta Oecol.* 20 (4), 267–283.
- Abrantes, K.G., Barnett, A., Bouillon, S., 2014. Stable isotope-based community metrics as a tool to identify patterns in food web structure in east African estuaries. *Funct. Ecol.* 85, 270–282.
- Allen, J., 1985. Field measurement of longshore sediment transport sandy hook, New Jersey, USA. *J. Coast. Res.* 1, 231–240.
- Allen, A., Gillooly, J., Brown, J., 2005. Linking the global carbon cycle to individual metabolism. *Funct. Ecol.* 19, 202–213.



- Andersen, T., et al., 2010. Erodibility of a mixed mudflat dominated by microphytobenthos and *Cerastoderma edule*, East Frisian Wadden Sea, Germany. *Estuar. Coast. Shelf Sci.* 87, 197–206.
- Anderson, M., 2008. Animal–sediment relationships re-visited: characterising species' distributions along an environmental gradient using canonical analysis and quantile regression splines. *J. Exp. Mar. Biol. Ecol.* 366, 16–27.
- Basset, A., Cozzoli, F., Paparella, F., 2012a. A unifying approach to allometric scaling of resource ingestion rates under limiting conditions. *Ecosphere* 3, 2.
- Basset, A., et al., 2012b. A benthic macroinvertebrate size spectra index for implementing the Water Framework Directive in coastal lagoons in Mediterranean and Black Sea ecoregions. *Ecol. Indic.* 12 (1), 72–83.
- Bates, D., Maechler, M., Bolker, S., Walker, S., 2015. Fitting linear mixed-effects models using lme4. *J. Stat. Softw.* 67, 1–48.
- Beukema, J., de Vlas, J., 1979. Population parameters of the lugworm, *Arenicola marina*, living on tidal flats in the Dutch Wadden Sea. *Neth. J. Sea Res.* 13, 331–353.
- Bolker, B., et al., 2009. Generalized linear mixed models: a practical guide for ecology and evolution. *Trends Ecol. Evol.* 24, 127–135.
- Bouma, T., et al., 2014. Identifying knowledge gaps hampering application of intertidal habitats in coastal protection: Opportunities & steps to take. *Coast. Eng.* 87, 147–157.
- Brey, T., 2001. Population dynamics in benthic invertebrates. [Online] Available at: <http://www.thomas-brey.de/science/>.
- Brey, T., 2010. An empirical model for estimating aquatic invertebrate respiration. *Methods Ecol. Evol.* 1, 92–101.
- Briggs, K., Cartwright, G., Friedrichs, C., Shivarudruppa, S., 2015. Biogenic effects on cohesive sediment erodibility resulting from recurring seasonal hypoxia on the Louisiana shelf. *Cont. Shelf Res.* 93, 17–26.
- Brock, J., et al., 2006. Northern Florida reef tract benthic metabolism scaled by remote sensing. *Mar. Ecol. Prog. Ser.* 312, 123–139.
- Brown, J., et al., 2004. Toward a metabolic theory of ecology. *Ecology* 82, 1771–1789.
- Brown, J., Allen, A., Gillooly, J., 2007. The metabolic theory of ecology and the role of body size in marine and freshwater ecosystems. *Body Size: the Structure and Function of Aquatic Ecosystems*. Cambridge University Press, Cambridge, pp. 1–15.
- Canavero, A., Hernández, D., Zarucki, M., Arim, A., 2014. Patterns of co-occurrences in a killifish metacommunity are more related with body size than with species identity. *Aust. Ecol.* 39, 455–461.
- Chen, X., et al., 2017. Bioturbation as a key driver behind the dominance of Bacteria over Archaea in near-surface sediment. *Sci. Rep.* 7.
- Ciutat, A., Widdows, J., Pope, N., 2007. Effect of *Cerastoderma edule* density on near-bed hydrodynamics and stability of cohesive muddy sediments. *J. Exp. Mar. Biol. Ecol.* 346 (1–2), 114–126.
- Clarck, A., 2006. Temperature and the metabolic theory of ecology. *Funct. Ecol.* 20, 405–412.
- Clark, A., Johnston, N., 1999. Scaling of metabolic rate with body mass and temperature in teleost fish. *J. Anim. Ecol.* 68, 893–905.
- Cozzoli, F., Bouma, T., Ysebaert, T., Herman, P., 2013. Application of non-linear quantile regression to macrozoobenthic species distribution modelling: comparing two contrasting basins. *Mar. Ecol. Prog. Ser.* 475, 119–133.
- Cozzoli, F., et al., 2014. A mixed modeling approach to predict the effect of environmental modification on species distributions. *PLoS One* 9, e89131.
- Cozzoli, F., et al., 2017. A modeling approach to assess coastal management effects on benthic habitat quality: a case study on coastal defense and navigability. *Estuar. Coast. Shelf Sci.* 184, 67–82.
- Cozzoli, F., et al., 2018a. The combined influence of body size and density on cohesive sediment resuspension by bioturbators. *Sci. Rep.* 8 (3831), 12.
- Cozzoli, F., Ligetta, G., Vignes, F., Basset, A., 2018b. Revisiting GUD: an empirical test on size-dependencies of patch exploitation behaviour. *PLoS One* 13 (9), e0204448.
- Cozzoli, F., Gjoni, V., Basset, A., 2019. Size dependence of patch departure behavior: evidence from granivorous rodents. *Ecology* (In press).
- Crooks, J., 2002. Characterizing ecosystem-level consequences of biological invasions: the role of ecosystem engineers. *Oikos* 97, 153–166.
- Daggers, T., Kromkamp, J., Herman, P., Van Der Wal, D., 2018. A model to assess microphytobenthic primary production in tidal systems using satellite remote sensing. *Remote Sens. Environ.* 211, 129–145.
- Damuth, J., 1991. Ecology - of size and abundance. *Nature* 351, 268–269.
- David, V., et al., 2016. Impact of biofilm resuspension on mesozooplankton in a shallow coastal ecosystem characterized by a bare intertidal mudflat. *J. Mar. Biol. Assoc. UK* 96, 1319–1329.
- De Backer, A., et al., 2011. Bioturbation effects of *Corophium volutator*: importance of density and behavioural activity. *Estuar. Coast. Shelf Sci.* 91, 306–313.
- de Deckere, E., van de Koppel, J., Heip, C., 2000. The influence of *Corophium volutator* abundance on resuspension. *Hydrobiologia* 426, 37–42.
- De Roos, A., Persson, L., McCauley, E., 2003. The influence of size-dependent life-history traits on the structure and dynamics of populations and communities. *Ecol. Lett.* 6, 473–487.
- Degraer, S., et al., 2006. The Macrobenthos Atlas of the Belgian Part of the North Sea. Belgian Science Policy, Brussel.
- Donadi, S., et al., 2013. Cross-habitat interactions among bivalve species control community structure on intertidal flats. *Ecology* 94, 489–498.
- Dupont, E., Stora, G., Tremblay, P., Gilbert, F., 2006. Effects of population density on the sediment mixing induced by the gallery-diffuser *Hediste* (*Nereis*) *diversicolor* O.F. Müller, 1776. *Journal of Experimental Marine Biology and Ecology*. *J. Exp. Mar. Biol. Ecol.* 336 (1), 33–41.
- Edgar, G., 1993. Measurement of the carrying capacity of benthic habitats using a metabolic-rate based index. *Oecologia* 95 (1), 115–121.
- Ernest, S., et al., 2003. Thermodynamic and metabolic effects on the scaling of production and population energy use. *Ecol. Lett.* 6, 990–999.
- Fagherazzi, S., Wiberg, P., 2009. Importance of wind conditions, fetch, and water levels on wave-generated shear stresses in shallow intertidal basins. *J. Geophys. Res.* 114, F03022.
- Fernandes, S., Sobral, P., Costa, M., 2006. *Nereis diversicolor* effect on the stability of cohesive intertidal sediments. *Aquat. Ecol.* 40, 567–579.
- Flach, E., 1996. The influence of the cockle, *Cerastoderma edule*, on the macrozoobenthic community of tidal flats in the Wadden Sea. *Mar. Ecol. Prog. Ser.* 17 (1), 87–98.
- Friedrichs, C., 2011. Tidal flat morphodynamics. In: Wolanski, E., McLusky, D. (Eds.), *Treatise on Estuarine and Coastal Science*. Elsevier, p. 4590 s.l.
- Friedrichs, M., Leipe, T., Peine, F., Graf, G., 2009. Impact of macrozoobenthic structures on near-bed sediment fluxes. *J. Mar. Syst.* 75, 336–347.
- Gaston, K., Blackburn, T., 2000. *Pattern and Process in Macroecology*. s.l. Blackwell Science.
- Gerdol, V., Hughes, R., 1994. Feeding behaviour and diet of *Corophium volutator* in an estuary in southeastern England. *Mar. Ecol. Prog. Ser.* 114, 103–108.
- Gillooly, J., et al., 2001. Effects of size and temperature on developmental time. *Nature* 417, 70–73.
- Gillooly, J., et al., 2006. Response to Clarke and Fraser: effects of temperature on metabolic rate. *Funct. Ecol.* 20 (2), 400–404.
- Gjoni, V., Basset, A., 2018. A cross-community approach to energy pathways across lagoon macroinvertebrate guilds. *Estuar. Coasts* 41 (8), 2433–2446.
- Gjoni, V., Cozzoli, F., Rosati, I., Basset, A., 2017. Size–density relationships: a cross-community approach to benthic macroinvertebrates in Mediterranean and Black Sea Lagoons. *Estuar. Coasts* 40 (4).
- Glazier, D., 2005. Beyond the '3/4-power law': variation in the intra- and interspecific scaling of metabolic rate in animals. *Biol. Rev.* 80, 611–662.
- Glazier, D., et al., 2011. Ecological effects on metabolic scaling: amphipod responses to fish predators in freshwater springs. *Ecol. Monogr.* 81 (4), 599–618.
- Grabowski, R., Droppo, I., Wharton, G., 2011. Erodibility of cohesive sediment: the importance of sediment properties. *Earth Sci. Rev.* 105 (3–4), 101–120.
- Grömping, U., 2006. Relative importance for linear regression in R: the package relaimp. *J. Stat. Softw.* 17 (1), 1–27.
- Guelorget, O., Perthuisot, J., 1992. Vie et Milieu. *Paralic Ecosystems. Biological Organization and Functioning*. 42 pp. 215–251.
- Hedman, J., Gunnarsson, J., Samuelsson, G., Gilbert, F., 2011. Particle reworking and solute transport by the sediment-living polychaetes *Marenzelleria neglecta* and *Hediste diversicolor*. *J. Exp. Mar. Biol. Ecol.* 407 (2), 294–301.
- Holtmann, S., et al., 1996. *Atlas of the Zoobenthos of the Dutch Continental Shelf*. Ministry of Transport, Public Works and Water Management Rijkswaterstaat, Amsterdam.
- Hu, Z., et al., 2015. Predicting long-term and short-term tidal flat morphodynamics using a dynamic equilibrium theory. *J. Geophys. Res. Earth Surf.* 120, 1803–1823.
- Hu, Z., Van Der Wal, D., Cai, H., Van Belzen, J., Bouma, T.J., 2018. Dynamic equilibrium behaviour observed on two contrasting tidal flats from daily monitoring of bed-level changes. *Geomorphology* 311, 114–126.
- Humphreys, J., et al., 2015. Introduction, dispersal and naturalization of the Manila clam *Ruditapes philippinarum* in British estuaries, 1980–2010. *J. Mar. Biol. Assoc. UK* 95 (6), 1163–1172.
- Humphries, M., McCann, K., 2014. Metabolic ecology. *J. Anim. Ecol.* 83 (1), 7–19.
- Ileno, E., Solan, M., Batty, P., Pierce, G., 2006. How biodiversity affects ecosystem functioning: roles of infaunal species richness, identity and density in the marine benthos. *Mar. Ecol. Prog. Ser.* 311, 263–271.
- Joensuu, M., et al., 2018. Sediment properties, biota, and local habitat structure explain variation in the erodibility of coastal sediments. *Limnol. Oceanogr.* 63, 173–186.
- Jones, C., Lawton, J., Shachak, M., 1994. Organisms as ecosystem engineers. *Oikos* 69 (3), 373–386.
- Jones, C., Lawton, J., Shachak, M., 1997. Positive and negative effects of organisms as physical ecosystem engineers. *Ecology* 78 (7), 1946–1957.
- Kleiber, M., 1932. Body size and metabolism. *Hilgardia* 6, 315–353.
- Kooijman, S., 2000. *Dynamic Energy and Mass Budgets in Biological Systems*. Cambridge University Press, Cambridge.
- Kristensen, E., 1983. Ventilation and oxygen uptake by 3 species of *Nereis* (Annelida: Polychaeta). II. Effects of temperature and salinity changes. *Mar. Ecol. Prog. Ser.* 12, 299–306.
- Kristensen, E., 2001. Impact of polychaetes (*Nereis* spp. and *Arenicola marina*) on carbon biogeochemistry in coastal marine sediments. *Geochim. Trans.* 2, 92–103.
- Kristensen, E., et al., 2013. Influence of benthic macroinvertebrates on the erodibility of estuarine cohesive sediments: Density- and biomass-specific responses. *Estuar. Coast. Shelf Sci.* 134, 80–87.
- Kupryianchuk, D., et al., 2013. Bioturbation and dissolved organic matter enhance contaminant fluxes from sediment treated with powdered and granular activated carbon. *Environ. Sci. Technol.* 47 (10), 5092–5100.
- Le Hir, P., Monbet, Y., Orvain, F., 2007. Sediment erodibility in sediment transport modelling: Can we account for biota effects? *Cont. Shelf Res.* 27, 1116–1142.
- Lee, H., Swartz, R., 1980. Biological processes affecting the distribution of pollutants in marine sediments. Part II. Biodeposition and bioturbation. In: Baker, R. (Ed.), *Contaminants and Sediment*. Environmental Protection Agency s.l.
- Li, B., et al., 2017. Bioturbation effect on the erodibility of cohesive versus non-cohesive sediments along a current velocity gradient: a case study on cockles. *J. Exp. Mar. Biol. Ecol.* 496, 84–90.
- Lindeman, R., Merenda, P., Gold, R., 1980. *Introduction to Bivariate and Multivariate Analysis*. Scott, Foresman, Glenview (IL).
- Maire, O., et al., 2006. Effects of food availability on sediment reworking in *Abra ovata* and *A. nitida*. *Mar. Ecol. Prog. Ser.* 319, 135–153.
- Marquet, P., et al., 2005. Scaling and power-laws in ecological systems. *J. Exp. Biol.* 208, 1749–1769.



- McGill, B., Enquist, B., Weiher, E., Westoby, M., 2006. Rebuilding community ecology from functional traits. *Trends Ecol. Evol.* 21 (4), 78–185.
- Meadows, P., Reid, A., 1966. The behaviour of *Corophium volutator* (Crustacea: Amphipoda). *J. Zool.* 150, 387–399.
- Meadows, P., Tait, J., 1989. Modification of sediment permeability and shear strength by two burrowing invertebrates. *Mar. Biol.* 101, 75–82.
- Meadows, P., Tait, J., Hussain, S., 1990. Effects of estuarine infauna on sediment stability and particle sedimentation. *Hydrobiologia* 190, 263–266.
- Mehta, A., Partheniades, E., 1982. Resuspension of Deposited Cohesive Sediment Beds. 18th Conference on Coastal Engineering ASCE, Cape Town.
- Menezes, S., Baird, D., Soares, A., 2010. Beyond taxonomy: a review of macroinvertebrate trait-based community descriptors as tools for freshwater biomonitoring. *J. Appl. Ecol.* 47 (4), 711–719.
- Mermillod-Blondin, F., Lemoine, D.G., 2010. Ecosystem engineering by tubificid worms stimulates macrophyte growth in poorly oxygenated wetland sediments. *Funct. Ecol.* 24, 444–453.
- Montserrat, F., et al., 2008. Benthic community-mediated sediment dynamics. *Mar. Ecol. Prog. Ser.* 372, 43–59.
- Montserrat, F., et al., 2009. Sediment segregation by biodiffusing bivalves. *Estuar. Coast. Shelf Sci.* 83 (4), 379–391.
- Mouillot, D., et al., 2006. Alternatives to taxonomic-based approaches to assess changes in transitional water communities. *Aquat. Conserv.* 16, 469–482.
- Nascimento, I., Dickson, K., Zimmerman, E., 1996. Heat shock protein response to thermal stress in the Asiatic clam, *Corbicula fluminea*. *Aquat. Ecosyst. Health* 5 (4), 231–238.
- Nasermoaddeli, M., et al., 2018. A model study on the large-scale effect of macrofauna on the suspended sediment concentration in a shallow shelf sea. *Estuar. Coast. Shelf Sci.* 211, 62–76.
- Nilsson, H., Rosenberg, R., 2002. Succession in marine benthic habitats and fauna in response to oxygen deficiency: analysed by sediment profile-imaging and by grab samples. *Mar. Ecol. Prog. Ser.* 197, 139–149.
- Ong, E., Briff, M., Moens, T., Van Colen, C., 2017. Physiological responses to ocean acidification and warming synergistically reduce condition of the common cockle *Cerastoderma edule*. *Mar. Environ. Res.* 130, 38–47.
- Orvain, F., 2005. A model of sediment transport under the influence of surface bioturbation: generalisation to the facultative suspension-feeder *Scrobicularia plana*. *Mar. Ecol. Prog. Ser.* 286, 43–56.
- Orvain, F., Le Hir, P., Sauriau, P., 2003. A model of fluff layer erosion and subsequent bed erosion in the presence of the bioturbator, *Hydrobia ulvae*. *J. Mar. Res.* 61, 823–851.
- Orvain, F., Le Hir, P., Sauriau, P.G., S., L., 2012. Modelling the effects of macrofauna on sediment transport and bed elevation: Application over a cross-shore mudflat profile and model validation. *Estuar. Coast. Shelf Sci.* 108, 64–75.
- Pearce, T., 2011. Ecosystem engineering, experiment, and evolution. *Biol. Philos.* 26, 793–812.
- Pearson, T., Rosenberg, R., 1978. Macrobenthic succession in relation to organic enrichment and pollution of the marine environment. *Oceanogr. Mar. Biol. Annu. Rev.* 5, 229–311.
- Peters, R., 1983. *The Ecological Implications of Body Size*. Cambridge University Press, New York.
- Porter, E., Owens, M., Cornwell, J., 2006. Effect of sediment manipulation on the biogeochemistry of experimental sediment systems. *J. Coast. Res.* 22 (6), 1539–1551.
- Pörtner, H., Farrell, P., 2008. Physiology and climate change. *Science* 332 (5902), 690–692.
- Purchon, R., 1997. *The Biology of Mollusca*. 2nd edition. Pergamon Press Ltd. s.l.
- Queirós, A., et al., 2013. A bioturbation classification of European marine infaunal invertebrates. *Ecol. Evol.* 3 (11), 3958–3985.
- Queirós, A., et al., 2015. Can benthic community structure be used to predict the process of bioturbation in real ecosystems? *Prog. Oceanogr.* 137, 559–569.
- Quintana, C.O., Shimabukuro, M., Pereira, C.O., Alves, B.G., Moraes, P.C., Valdemarsen, T., Kristensen, E., Sumida, P.Y., 2015. Carbon mineralization pathways and bioturbation in coastal Brazilian sediments. *Sci. Rep.* 5, 16122.
- Rakotomalala, C., et al., 2015. Modelling the effect of *Cerastoderma edule* bioturbation on microphytobenthos resuspension towards the planktonic food web of estuarine ecosystem. *Ecol. Model.* 316, 155–167.
- Rasmussen, E., 1973. Systematics and ecology of the Isefjord marine fauna (Denmark). *Ophelia* 11, 1–507.
- R-Core-Team, 2017. *R: A Language and Environment for Statistical Computing*. R Foundation for Statistical Computing, Vienna, Austria <https://www.R-project.org/>.
- Roberts, W., Le Hir, P., Whitehouse, R., 2000. Investigation using simple mathematical models of the effect of tidal currents and waves on the profile shape of intertidal mudflats. *Cont. Shelf Res.* 20 (10–11), 1079–1097.
- Saint-Béat, B., et al., 2014. How does the resuspension of the biofilm alter the functioning of the benthos–pelagos coupled food web of a bare mudflat in Marennes-Oléron Bay (NE Atlantic). *J. Sea Res.* 92, 144–157.
- Savage, V., et al., 2004. Effects of body size and temperature on population growth. *Am. Nat.* 163, 429–441.
- Sgro, L., Mistri, M., Widdows, J., 2005. Impact of the infaunal Manila clam, *Ruditapes philippinarum*, on sediment stability. *Hydrobiologia* 550 (1), 175–182.
- Solan, M., et al., 2004a. Extinction and ecosystem function in the marine benthos. *Science* 306, 1177–1180.
- Solan, M., et al., 2004b. In situ quantification of bioturbation using time lapse fluorescent sediment profile imaging (fSPI), luminophore tracers and model simulation. *Mar. Ecol. Prog. Ser.* 271, 1–12.
- Sousa, T., Domingos, T., Kooijman, S., 2008. From empirical patterns to theory: a formal metabolic theory of life. *Philos. Trans. R. Soc. Lond. B* 363, 2453–2464.
- Sutherland, T., Grant, J., 1998. The effect of carbohydrate production by the diatom *Nitzschia curvilineata* on the erodibility of sediment. *Limnol. Oceanogr.* 41 (1), 65–72.
- Suykerbuyk, W., et al., 2012. Suppressing antagonistic bio-engineering feedbacks doubles restoration success. *Ecol. Appl.* 22, 1224–1231.
- Swartz, L., 1991. Seasonal variation in body weight of the bivalves *Macoma balthica*, *Scrobicularia plana*, *Mya arenaria* and *Cerastoderma edule* in the Dutch Wadden sea. *Neth. J. Sea Res.* 28 (3), 231–245.
- Tagliapietra, D., Sigovini, M., Magni, P., 2012. Saprobity: a unified view of benthic succession models for coastal lagoons. *Hydrobiologia* 686 (1), 15–28.
- Thomsen, M., et al., 2017. Consequences of biodiversity loss diverge from expectation due to post-extinction compensatory responses. *Sci. Rep.* 7.
- Thrush, S., Hewitt, J., Herman, P., 2005. Multi-scale analysis of species–environment relationships. *Mar. Ecol. Prog. Ser.* 302, 13–26.
- Tolhurst, T., et al., 2006. Small-scale temporal and spatial variability in the erosion threshold and properties of cohesive intertidal sediments. *Cont. Shelf Res.* 26 (3), 351–362.
- Ubertini, M.L.S., Gangnery, A., Grangere, K., LeGendre, R.O.F., 2012. Spatial variability of benthic–pelagic coupling in an estuary ecosystem: consequences for microphytobenthos resuspension phenomenon. *PLoS One* 7.
- Valdemarsen, T., Quintana, C.O., Thorsen, S.W., Kristensen, E., 2018. Benthic macrofauna bioturbation and early colonization in newly flooded coastal habitats. *PLoS one* 13 (4), e0196097.
- van der Meer, J., et al., 2013. Measuring the flow of energy and matter in marine benthic animal populations. In: Eleftheriou, A. (Ed.), *Methods for the Study of Marine Benthos*. John Wiley & Sons, pp. 326–407 s.l.
- van Prooijen, B., Winterwerp, J., 2010. A stochastic formulation for erosion of cohesive sediments. *J. Geophys. Res.* 115 (C01005).
- van Prooijen, B., Montserrat, F., Herman, P., 2011. A process-based model for erosion of *Macoma balthica*-affected mud beds. *Cont. Shelf Res.* 31, 527–538.
- van Wesenbeeck, B., et al., 2007. Biomechanical warfare in ecology: negative interactions between species by habitat modification. *Oikos* 116, 742–750.
- Vannote, R., et al., 1980. The river continuum concept. *Can. J. Fish. Aquat. Sci.* 37, 130–137.
- Verdelhos, T., Marques, J., Anastácio, P., 2015a. Behavioral and mortality responses of the bivalves *Scrobicularia plana* and *Cerastoderma edule* to temperature, as indicator of climate change's potential impacts. *Ecol. Indic.* 58, 95–103.
- Verdelhos, T., Marques, J., Anastácio, P., 2015b. The impact of estuarine salinity changes on the bivalves *Scrobicularia plana* and *Cerastoderma edule*, illustrated by behavioral and mortality responses on a laboratory assay. *Ecol. Indic.* 52, 96–104.
- Volkenborn, N., Robertson, D., Reise, K., 2009. Sediment destabilizing and stabilizing bio-engineering on tidal flats: cascading effects of experimental exclusion. *Helgol. Mar. Res.* 63, 27–35.
- Vos, P., Misdorp, R., De Boer, P., 1998. Sediment stabilization by benthic diatoms in intertidal sandy shoals: qualitative and quantitative observations. In: D. B., P., van Gelder, A., Nio, S. (Eds.), *Tide-Influenced Sedimentary Environments and Facies*. Reidel, pp. 511–526 s.l.
- Walles, B., et al., 2015. The ecosystem engineer *Crassostrea gigas* affects tidal flat morphology beyond the boundary of their reef structures. *Estuar. Coast.* 38, 941–959.
- Wendelboe, K., Egelund, J., Mogens, R., Valdemarsen, T., 2013. Impact of lugworms (*Arenicola marina*) on mobilization and transport of fine particles and organic matter in marine sediments. *J. Sea Res.* 76, 31–38.
- Widdows, J., Brinsley, M., 2002. Impact of biotic and abiotic processes on sediment dynamics and the consequences to the structure and functioning of the intertidal zone. *J. Sea Res.* 48 (2), 143–156.
- Widdows, J., Brinsley, M., Salkeld, P., Elliott, M., 1998. Use of annular flumes to determine the influence of current velocity and bivalves on material flux at the sediment–water interface. *Estuaries* 21, 552–559.
- Widdows, J., Brinsley, M., Pope, N., 2009. Effect of *Nereis diversicolor* density on the erodibility of estuarine sediment. *Mar. Ecol. Prog. Ser.* 378, 135–143.
- Willows, R., Widdows, J., Wood, R., 1998. Influence of an infaunal bivalve on the erosion of an intertidal cohesive sediment: a flume and modeling study. *Limnol. Oceanogr.* 43, 1332–1343.
- Winterwerp, J., van Kesteren, W., 2004. *Introduction to the Physics of Cohesive Sediment in the Marine Environment*. Elsevier, Amsterdam.
- Winterwerp, J., et al., 2018. Efficient consolidation model for morphodynamic simulations in low-SPM environments. *J. Hydraul. Eng.* 144 (8), 04018055.
- Wrede, A., et al., 2018. Organism functional traits and ecosystem supporting services – a novel approach to predict bioirrigation. *Ecol. Indic.* 91, 737–743.
- Ysebaert, T., Herman, P., 2002. Spatial and temporal variation in benthic macrofauna and relationships with environmental variables in an estuarine, intertidal soft-sediment environment. *Mar. Ecol. Prog. Ser.* 244, 105–124.
- Yvon-Durocher, G., et al., 2012. Reconciling the temperature dependence of respiration across timescales and ecosystem types. *Nature* 487, 472–473.
- Zebe, E., Schiedek, D., 1996. The lugworm *Arenicola marina*: a model of physiological adaptation to life in intertidal sediments. *Helgolander Meeresunters* 50, 37–68.
- Zhang, L., et al., 2017. The impact of deep-tier burrow systems in sediment mixing and ecosystem engineering in early Cambrian carbonate settings. *Sci. Rep.* 7.
- Zhou, Z., et al., 2015. Modeling sorting dynamics of cohesive and non-cohesive sediments on intertidal flats under the effect of tides and wind waves. *Cont. Shelf Res.* 104, 76–91.
- Zhu, Z., et al., 2016. Interactive effects between physical forces and ecosystem engineers on seed burial: a case study using *Spartina anglica*. *Oikos* 125 (1), 98–106.
- Zou, K., Thébaud, E., Lacroix, G., Barot, S., 2016. Interactions between the green and brown food web determine ecosystem functioning. *Funct. Ecol.* 30, 1454–1465.
- Zuur, A., et al., 2009. *Mixed Effects Models and Extensions in Ecology*. Springer-Verlag, New York.
- Zwarts, L., Wanink, J., 1989. Siphon size and burying depth in deposit- and suspension-feeding benthic bivalves. *Mar. Biol.* 100, 227–240.
- Zwarts, L., Blomert, A., Spaak, P., de Vries, B., 1994. Feeding radius, burying depth and siphon size of *Macoma balthica* and *Scrobicularia plana*. *J. Exp. Mar. Biol. Ecol.* 183 (2), 193–212.